THE ROLE OF THE IMMUNE SYSTEM IN MuSC AGING DURING REGENERATION

FILIPA NARCISO LAGOA

A dissertation submitted in partial fulfillment of the requirements for the Degree of Masters in Biomedical Research (Specialization Area: Aging and Chronic Diseases) at Faculdade de Ciências Médicas | NOVA Medical School of NOVA University Lisbon

September, 2023

THE ROLE OF THE IMMUNE SYSTEM IN MuSC AGING DURING REGENERATION

Filipa Narciso Lagoa

Supervisors:
Dr Pedro Sousa-Victor, Principal Investigator at Instituto de Medicina Molecular,
Dra Joana Mendes Neves, Principal Investigator at Instituto de Medicina Molecular,
Dra Sílvia Vilares Conde, Associate Professor at Nova Medical School

A dissertation submitted in partial fulfillment of the requirements for the Degree of Masters in Biomedical Research (Specialization Area: Ageing and Chronic Diseases)

September, 2023

“The most beautiful experience we can have is the mysterious. It is the fundamental emotion that stands at the cradle of true art and true science.”

-Albert Einstein

Funding

The source of funding for this project comes from the project EMBO IG 4448

Acknowledgements

Este ano, apesar de ter sido uma das melhores experiências que já vivi foi sem dúvida um dos anos mais desafiantes de sempre. Felizmente uma caminhada como esta não se faz sozinho, e por isso, queria agradecer nos próximos parágrafos a todas as pessoas que me ajudaram ao longo deste percurso.

Em primeiro lugar quero agradecer ao **Doutor Pedro Sousa-Victor** e **Doutora Joana Neves** por me aceitarem no laboratório "Aging and Tissue Repair" e por toda a paciência que tiveram comigo. Desde ensinarem-me diversos protocolos, darem-me a oportunidade de crescer no meu próprio ritmo até semanalmente dispensarem um pouco do seu tempo para me orientar no meu projeto. Foi um privilégio crescer convosco e trabalhar no incrível ambiente do Instituto de Medicina Molecular.

Aos meus colegas do laboratório, **Margarida**, **Isabel**, **Mariana**, **Linde**, **Inês Martins**, **Tiago** pelos momentos bonitos que criámos juntos, pelas partilhas, conversas e aquele pedacinho de chocolate que ajudaram nas alturas mais stressantes neste último ano. Em especial quero agradecer à **Neuza** por toda disponibilidade e paciência que teve para me auxiliar na minha tese, pois mesmo quando estava mais atarefada com o seu projeto nunca me deixou "sozinha". À **Inês Antunes** por cuidar dos meus ratinhos e sacrificá-los para este projeto. À **Beatriz Jorge** pela amizade, pelas conversas, partilhas e inúmeros chocolates quentes que tornaram tudo mais divertido e memorável.

Às minhas amigas **Ana** e **Bea** que me acompanharam mais de perto neste percurso. Obrigada por todo o apoio, carinho, gargalhadas e por me ouvirem de coração aberto quando mais precisei. É um privilégio poder continuar a crescer ao vosso lado.

Aos meus colegas de mestrado, **Inês Justo, Maria, Madalena** por estarem sempre lá para mim e em especial à **Bárbara** por todos os cafés, partilhas, abraços e sorrisos que tornavam sempre qualquer dia menos bom num dia incrível.

Aos meus amigos de leiria especialmente à **Francisca, Ana, Adriana e Pedro** por me ajudarem a recarregar energias ao longo do ano e por me darem aquele bocadinho extra de força e de motivação.

Aos meus amigos da música, aos **colegas**, aos **coros** que acompanho e aos **meus alunos**, obrigada por abrilhantarem os meus fins de semana com muita música, animação e sempre muitas gargalhadas.

Por último, mas um dos principais agradecimentos que tenho a fazer é à **minha família** por todo o apoio e amor que me dão constantemente. Não imaginam o orgulho que tenho de poder dizer que vos tenho do meu lado. **Mana, mãe, tios, primos** e **avós** obrigada por acreditarem sempre em mim e por me darem tanta força para conquistar os meus objetivos. Em especial quero agradecer ao **meu pai**, o meu herói, obrigada por seres a melhor pessoa que conheço, por me ensinares o que é a verdadeira felicidade, e por me dares o teu ombro e os teus conselhos ao longo deste ano. **Pai**, consegui sou mestre!

A todos vocês, muito obrigada, fizeram com que tudo valesse apena

Abstract

Age-related loss of regenerative capacity in the skeletal muscle is associated with a reduction in myeloid cells in the regenerating tissue, diminished muscle stem cell (MuSC) populations, and intrinsic defects within the remaining MuSCs. However, the consequences of the age-related immune alterations on MuSCs remain a subject of investigation.

Preliminary investigations in both aged mice and mouse models of immune aging (that mimic age-related reductions in myeloid populations), have shown a dual phenomenon occurring during regeneration involving a reduction in MuSC numbers and the conversion of MuSCs into a distinct subpopulation characterized by the expression of Sca-1. Transcriptomic analysis of this new MuSC population showed a link with interferon (IFN) responses. This project aims to investigate the immune system's role in MuSC aging during regeneration and study the potential impact of IFN signaling on MuSC's behavior during skeletal muscle regeneration in conditions of immune dysfunction.

In this work, we showed that in the absence of macrophages during regeneration, MuSCs disappear from the skeletal muscle due to an increase in cell death and a cell fate switch mechanism from α7Integrin^{pos}Sca-1^{neg} MuSCs to α7Integrin^{pos}Sca-1^{pos} MuSC population, both happening at 3dpi. Interferon alpha, but also Poly IC (an inducer of IFN signaling, mimicking cellular debris), administration *in vivo* were sufficient to induce the cell fate switch observed after macrophage ablation. Using *in vitro* experiments, we found that IFNα acts directly on MuSCs and the effects are mediated by the JAK-STAT pathway. Finally, we showed that the IFNα administration is sufficient to impair myofiber formation following regeneration.

With this work, we propose that the accumulation of cell debris after injury, in the absence of macrophages, activates an unknown cell to produce IFNα that stimulates the MuSC to switch from a α7Integrin^{pos}Sca-1^{neg} MuSC population into a α7Int^{pos}Sca-1^{pos} MuSC population, through the JAK-STAT pathway. We suggest a similar mechanism could mediate the cell fate switch of MuSCs in aging.

Keywords: Skeletal muscle, MuSCs aging, clodronate-treated mice, cell fate switch, Interferon alpha, α7Integrin^{pos}Sca-1^{pos}

Resumo

A perda de capacidade regenerativa relacionada à idade no músculo esquelético está associada a uma redução nas células mieloides no tecido em regeneração, à diminuição das populações de células estaminais musculares (MuSC) e acumulação de defeitos intrínsecos nas MuSCs remanescentes. No entanto, continuam por serem investigadas, as consequências das alterações imunológicas relacionadas com o envelhecimento nas MuSCs.

Investigações preliminares em ratinhos idosos e em modelos com defeitos imunológicos associados à idade que mimetizam o decréscimo na população mieloide, mostraram um fenômeno duplo durante a regeneração envolvendo uma redução no número de MuSCs e a conversão de uma porção de MuSCs numa subpopulação distinta caracterizada pela expressão de Sca-1. Análises transcriptómicas desta nova população de MuSC (α7Integrin^{pos}Sca-1^{pos}) mostraram uma conexão da população com genes relacionados com a resposta de interferão (IFN). Este projeto visa investigar o papel do sistema imunológico no envelhecimento de MuSCs durante a regeneração muscular, e estudar o potencial impacto do interferão no comportamento de MuSCs em regenerações musculares modificadas imunologicamente.

Neste trabalho, percebemos que na ausência de macrófagos durante a regeneração, as MuSCs desaparecem do músculo esquelético devido a dois fatores simultâneos a três dias após a regeneração: um aumento na morte celular das MuSCs e a um mecanismo de mudança de destino celular da população α7Int^{pos}Sca-1^{neg} para a população α7Int^{pos}Sca-1^{pos}. A administração *in vivo* de Interferon alfa (IFNα) mas também o Poly IC (um indutor da via de sinalização do interferão, mimetizando debris celular) foi suficiente para induzir a mudança do destino celular observada após a eliminação de macrófagos. Através de experiências *in vitro*, descobrimos que o IFNα atua diretamente nas MuSC e os efeitos são mediados pela via JAK-STAT. Finalmente, mostramos que a administração de IFNα é suficiente para prejudicar a formação miofibras após a regeneração.

Com a elaboração deste trabalho, propomos que o acúmulo de detritos celulares na ausência de macrófagos, ativa uma população celular desconhecida para produzir IFNα que estimula as MuSC a mudar de uma população α7Int^{pos}Sca-1^{neg} para uma população α7Int^{pos}Sca-1^{pos}, através da via JAK-STAT. Sugerimos que um mecanismo semelhante poderia mediar a mudança do destino celular das MuSCs no envelhecimento.

Palavras-chave: Músculo esquelético, MuSCs envelhecidas, ratinhos tratados com clodronate, mudança de destino celular, Interferon alfa, α7Int^{pos}Sca-1^{pos}

Index

List of Figures

List of Tables

List of Acronyms

α7Integrin - Alpha seven Integrin
ABCG2 - ATP-binding cassette super-family G member 2
ASCs - Activated Satellite Cells
BaCl2 - Barium Chloride
BMCs - Bone Marrow Cells
BMDMs - Bone Marrow-Derived Macrophages
C/EBP - CCAAT/enhancer binding protein
CCL2 - C-C Motif Chemokine Ligand 2
CCR2 - C-C Motif Chemokine Receptor 2
CD31 - Cluster of Differentiation 31
CD4 - Cluster of Differentiation 4
CD45 - Cluster of Differentiation 45
CD8 - Cluster of Differentiation 8
CX3CR1 - CX3C motif Chemokine Eeceptor 1
CXCL10 - C-X-C motif Chemokine Ligand 10
CXCR3 - receptor C-X-C motif Chemokine Receptor 3
DAMPs - Damage-Associated Molecular Patterns
DNA - Deoxyribonucleic Acid
Dpi - Day(s) Post Injury
ECM - Extracellular Matrix
FAPs - Fibro Adipogenic Progenitors
GAS - Gamma-Activated Sequence
GDF3 - Growth Differentiation Factor-3
HLH - Hemophagocytic Lymphohistiocytosis
ICDs - Intracellular Domains
IFN - Interferon
IFNa - Interferon alpha
IFNAR - Interferon-α/β Receptor
IFNGR - Interferon gamma Receptor
IFNLR - Interferon Lambda Receptor
IFNRMs - IFN-Responsive Macrophages
IFN-β - Interferon beta
IFNγ - Interferon gamma
IFN-ε - Interferon epsilon
IFN-κ - interferon kappa
IFN-λ - Interferon lambda
IFN-τ - Interferon tau
IFN-ω - Interferon omega

IL - Interleukin
IL-10 - Interleukin 10
IL10RB - Interleukin 10 Receptor Subunit Beta
IL-2 - Interleukin 2
IL-4 - Interleukin 4
IL6 - Interleukin 6
ILC1 - Innate lymphoid cel
ISGs - Interferon-Stimulated Genes
ISRE - interferon-Stimulated Response Element
JAK 1 - Janus Family Tyrosine Kinase 1
JAK 2 - Janus Family Tyrosine Kinase 2
JAK 3 - Janus Family Tyrosine Kinase 3
JAK-STAT - Janus Kinase/Signal Transducers and Activators of Transcription
LIF - Leukemia Inhibitory Factor
Ly6C - Lymphocyte antigen 6 family member C
Ly6G - Lymphocyte antigen 6 family member G
MCP-1 - Macrophage Chemoattractant Protein 1
MFRs - Muscle Regulatory Transcription Factors
MuSC - Muscle stem cell
MYF4 - Myogenic Factor 4
MYF5 - Myogenic Factor 5
MyHC - Myosin Heavy Chain
MYOD - Myogenic Differentiation
PAX3 - Paired Box3
PAX7 - Paired Box7
PD-1 - Programmed Death-1
Poly IC - Polyinosinic Polycytidylic Acid
Pos - Positive
PPARs - Peroxisome Proliferator Activated Receptors
QSC - Quiescent MuSC
RNA - Ribonucleic Acid
ROS - Reactive Oxygen Specie
SCA-1 - Stem Cell Antigen-1
SNPs - Single Nucleotide Polymorphisms
STAT 1 - Signal Transducer and Activator of Transcription 1
STAT 2 - Signal Transducer and Activator of Transcription 2
STAT 3 - Signal Transducer and Activator of Transcription 3
T reg - Regulatory T cells
TGF-β1 - Transforming Growth Factor Beta 1

TNFα - Tumor Necrosis Factor Alpha

TYK2 - Tyrosine Kinase 2

Wnt - Wingless-related Integration Site

Introduction

1. Introduction

1.1. Aging as a natural lifespan outcome

The global population over 65 is expected to rise from 761 million, one in ten people, in 2021 to 1.6 billion, six in ten people, in 2050. Population aging is an unavoidable global phenomenon. Accounting populational prolonged lives through efforts in medicine and research with declining birth ratios, aging is progressing fast and is a natural outcome of this demographic transition worldwide[1] (**Figure 1**).

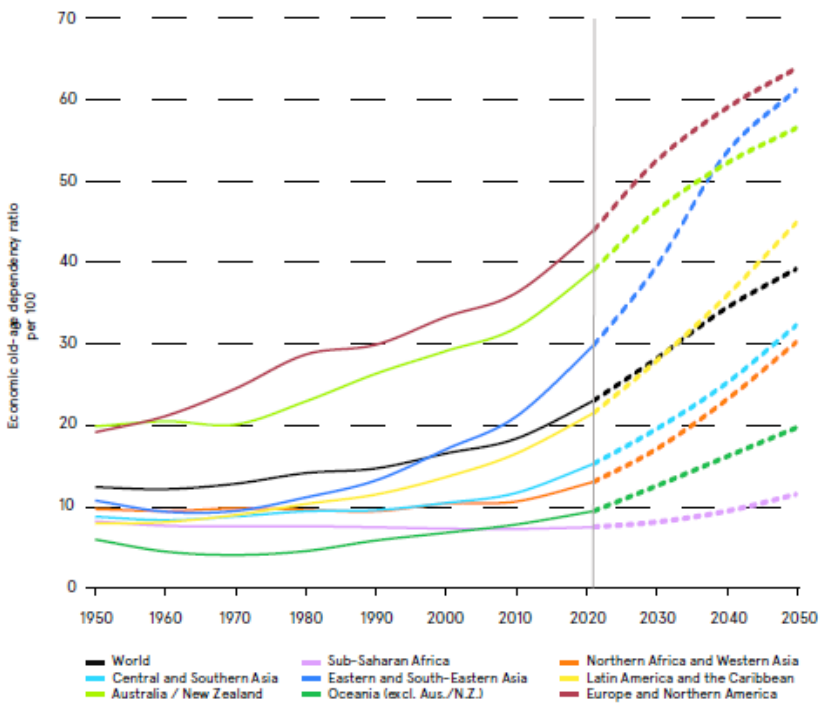

Figure 1. Worldwide statistics and predictions of people aged 65 years or over across the years. The Economic old-age dependency ratio refers to the number of ancient people (over 65 years old) that are not economically active in contrast with the number of people of the working age gap (18-64 years old). A low dependency ratio means the general population can support the aged population, and a high ratio indicates the opposite. The proportion of older people is increasing globally, and five out of eight regions will duplicate this ratio (Eastern and South-Eastern Asia, Latin America, the Caribbean, Central and Southern Asia, Northern Africa and Western Asia, and Oceania – excluding Australia and New Zealand). Between now and 2050, the world's oldest countries will change from Europe to Eastern to South-Eastern Asia. Image retrieved from[1]

Regardless of this projection, the increase in the older population percentage does not linearly correlate with health and well-being. The main concern related to population aging is a deterioration in the quality of life and an increase in chronic diseases and disabilities, impacting society and the economy[1,2].

Aging is a ubiquitous natural enduring process for all species resulting in a cumulative loss of physical health across all systems due to damage accumulation in response to various stimuli[2,3]. It is characterized by a decrease in tissue and cell functions and a significant increase in the risk of various aging-related diseases such as cardiovascular, neurodegenerative, musculoskeletal, metabolic, and immune system pathologies-related. These age-associated pathologies lead, in most scenarios, to the main causes of disabilities and death in the elderly. Despite all efforts towards aging research, the causes of aging - the external and internal triggers - still need to be clarified[2,3].

1.1.1. The New Hallmarks of Aging

The hallmarks of aging are processes or mechanisms observed during aging in which an experimental worsening must accelerate the aging process, and a bias improvement should delay it, enhancing healthy longevity[4]. According to this, in 2013, López-Otín and colleagues proposed nine hallmarks of aging subdivided into three main groups[4].

The first category has a negative aging impact and englobes genomic instability, telomere attrition, epigenetic alterations, and loss of proteostasis. Contrary to the first, the second group's function depends on its intensity. At low levels, these antagonistic hallmarks may be crucial for homeostasis; however, high levels provoke chronic instabilities. These factors are cellular senescence, mitochondrial dysfunction, and deregulated nutrient sensing. Finally, the third group, constituted by stem cell exhaustion and altered intercellular communication, is nominated as integrative hallmarks since it is an end-product of the previous first groups[4].

Ten years later, in Copenhagen, the "New Hallmarks of Ageing" symposium reviewed and approved five new hallmarks[5]: autophagy, dysregulation in ribonucleic acid (RNA) splicing, inflammation, loss of cytoskeleton integrity, and disturbance of the microbiome, completing a total of 13 hallmarks[5].

Although the hallmarks are stated individually when considered part of a network, they gain higher relevance in research and clinically[5]. Increased emphasis on the interconnection of multiple hallmarks is imperative, along with the more extensive use of systems biology methods for the future of aging research[5].

1.1.1.1. Inflammaging

Initially, inflammation was an element of the hallmark 'altered intercellular communication[4]. However, due to its significant interaction with cellular senescence[6] and the gut microbiota[7] (one of the new hallmarks of aging), with a substantial impact on aging, it was attributed to the hallmark recognition[5].

Inflammaging, or age-dependent chronic inflammation, is linked to a broad spectrum of aging-associated diseases like cardiovascular diseases, chronic morbidity, sarcopenia, cancer, and premature death[8]. Inflammaging characterizes by chronic high levels of proinflammatory cytokines in the blood,

such as interleukins IL-1, IL-6, C-reactive protein, IFNα, and others, linked to aging. Single nucleotide polymorphisms (SNPs) in the IL-6 promoter region leads to a baseline of IL-6 inflammatory continuous response that affects homeostasis[5].

The accumulation of damaged macromolecules, organelles, and cells in elderly organisms is a crucial trigger for continuous activation of the inflammatory signaling in aging[8]. Clearance strategies for hazardous products on the tissue are impaired in aging, leading to increased autonomous debris and free sequences of RNA lost in the tissue. Senescent cells and their inflammatory secretome in the tissue activate several proinflammatory mechanisms and pathways that have been the primary source of inflammation in aging[8].

Macrophages are the primary immune cell type responsible for tissue clearance due to their phagocytic capacity, and there are typically activated and concentrated after tissue injury[9]. In old organisms macrophage function declines and, given their importance in processes of tissue repair, regenerative capacity is affected by their defective function[9].

Model systems that allow the recapitulation of impaired immune system function in aging are fundamental to comprehend better the relationship between inflammatory signals, macrophage phenotypic switch, and the impact of those changes in other tissue cell types that help to coordinate regeneration like stem cells.

1.1.1.2. Stem Cell Exhaustion

The regenerative feature of the organisms depends on the stem cells' capacity to substitute deteriorated tissue[10]. Aging related-stem cell exhaustion results from broad crosstalk between multiple aging-associated damages affecting many intrinsic and extrinsic pathways leading to the deterioration of stem cell function[4]. The deficient proliferation of stem cells jeopardizes long-term regeneration compromising the individual's homeostasis. Nevertheless, overstimulation in stem cell proliferation can be responsible for stem cell niche depletion[4].

A stem cell niche is a microenvironment that communicates with stem cells and controls cell fate in response to specific external triggers[11]. Stem cells can differentiate into mature progeny and self-renew, making them long-lasting cells in the niche[11,12]. However, self-renewal potentiates the susceptibility of stem cells to accumulate genetic defects and cellular damage with aging, contributing to the loss of function, cell death, and senescence, impairing the stem cell function[11].

Regardless, discoveries of stem cell aging recuperation have generated curiosity concerning the creation of rejuvenating therapies that could positively impact stem cell niche and tissue regeneration[10]. Solutions targeting the aging-altered pathways in stem cell aging could be envisioned as viable strategies to improve the tissue's age-related dysfunction, rescuing some regeneration potential[10].

1.1.2. The Lack of Successful Regenerative Therapies

Regenerative medicine attempts to provide more and better rejuvenation strategies, acknowledging an aged worldwide population and a life quality decline, to improve lifespan and health by diminishing the age-related effects[2,13]. Over the years, scientists have unraveled several mechanisms influencing and deaccelerating aging in different animal models.

In 1925, it was found that the growth rate of *Drosophila* changes accordingly with the intensity of light. The higher the candlelight potency, the longer the larval period[14]. Besides, caloric restriction studies in mice have positively impacted those animals' longevity[15], and *Caenorhabditis elegans'* first long-lived strain found decades ago indicates that specific genes could be predisposed to a healthy aging process[16]. In humans, the challenge for enhancing this natural-continuous process is augmented. Human aging manifests as a multifactorial phenomenon that impairs the structure and function of the tissue and organs and facilitates other aged-related comorbidities to develop[2].

Although the aging-related impaired regeneration triggers remain unclear and can differ from organism to organism, the underlying changes associated with this process are well conserved across different species and tissues, suggesting the existence of common targets for intervention to improve regenerative capacity in the older population[10]. Environmental tissue modifications (locally and systematically), and stem cell ineffectiveness are the main aging-related changes affecting the regenerative ability of the tissues[13].

Stem cells are the primary pillar to restore tissue function, and many regenerative stem cell-based therapies rely on using endogenous stem cells or exogenous cells derived from stem cells to restore tissue degradation[10]. However, the efficacy of such therapeutic approaches is jeopardized by an age-related ineffective repair capacity to embrace them[10].

Regeneration success is determined by key inflammatory processes that are altered in aging and represent an obstacle to the effective transplant of stem cells[17]. The restitution of the regulated inflammatory pathways in aged organisms will improve the repaired tissue capacity through stimulating endogenous repair mechanisms, enhancing the success of stem cell-based therapies[8]. Identifying mechanisms that regulate immune system function during tissue regeneration and aging and have detrimental consequences for stem cells' endogenous function can reveal targets with clinical value to improve the repair capacity of old organisms[8,10].

1.2. Skeletal Muscle as a paradigm for Regeneration Research

Skeletal muscle is a highly flexible tissue that adapts to physiological demands such as development or activity, and it is known for its exceptional regenerating ability[18]. Outside of its capacity to regenerate,

skeletal muscle is also relatively accessible, with a wide range of experimental models that damage the tissue available[18]. It allows consecutive rounds of injury to study stem cell activity in the long term. Thus, skeletal muscle is one of the ideal tissues to investigate regeneration. Firstly, it is essential to distinguish skeletal muscle regeneration, repair, and remodeling.

Regeneration is a healing process that depends on an externally induced injury (physical or chemical) and is characterized by necrosis[17]. On the other hand, skeletal muscle repair refers to the mechanisms that allow the maintenance of the skeletal muscle mass during life in response to a temporary reduction in muscle strength, an increase in inflammatory response or an unaccustomed muscle contraction[17]. This temporary reduction in muscle strength provokes myofibrillar disruption with architectural changes that require repair, and this process is usually associated with humans[17]. While regeneration requires the replacement of muscle fibers, muscle repair involves the renewal of sections of fibers or individual sarcomeres. Remodeling is the capacity of the skeletal muscle to adapt to external stimuli like exercise[17].

1.2.1. From Function to Anatomy

Skeletal muscle is the most prominent tissue in the body, constituting 40% of the body weight in humans[19,20]. Skeletal muscle's primary assignments include producing movement, stabilizing the joints, sustaining body posture and position, regulating body temperature, and storing substrates such as amino acids and carbohydrates contributing to the basal energy metabolism as an endocrine organ[19,21]. In contrast to smooth and cardiac muscle contraction, nearly all skeletal muscle contraction occurs under voluntary control by brain inputs that enable conscious control of muscles[22].

The overall size of the muscle depends on the amount and dimensions of each muscle fiber. Skeletal muscle's architecture is schematized in **Figure 2** and is a unique alternate pattern between fibers and connective tissue (endomysium, perimysium, epimysium) that supports the myofibers to tolerate the stress of contraction[18,20].

The muscle fiber, an individual muscle cell known as the myofiber, is the smallest contractile unit of skeletal muscle[18,20]. It is a multinucleated cylindric-shaped elongated cell that contains mitochondria and sarcomeres[23]. Each muscle fiber is 100µm in diameter and 1 cm in length and is surrounded by the plasma membrane, the sarcolemma[20].

Each myofiber has billions of myofilaments (actin and myosin filaments), which are physically joined by various proteins found in the sarcolemma. The sarcomeres, the fundamental contractile units of skeletal muscle, are formed by assembling and organizing the myofilaments in a specific pattern[23].

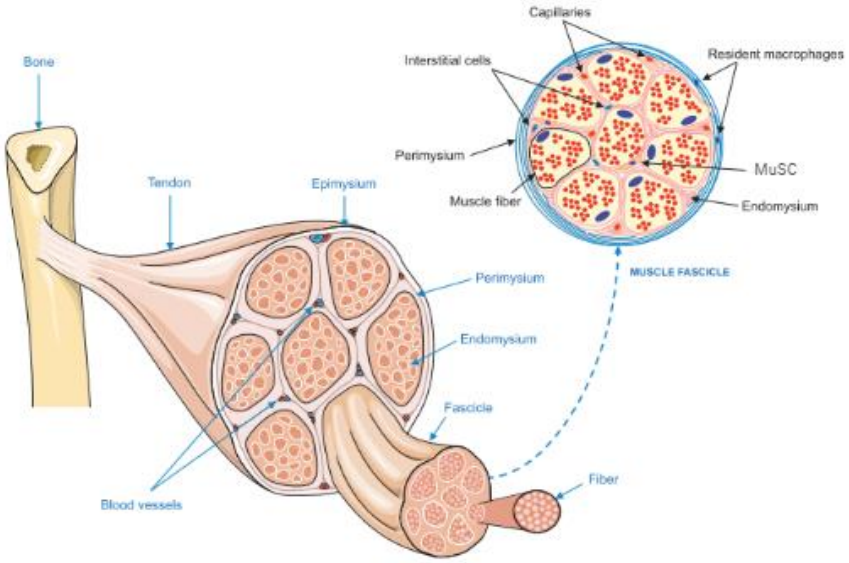

Figure 2. Skeletal Muscle architecture. The muscle is surrounded by the epimysium that extends from the tendons, which are attached to the bone. Within this external layer are fascicle groups involved in the intermedia connective, the perimysium. Nerves and blood vessels penetrate through the epimysium and travel into the perimysium. The bundles comprise several parallel fibers, each surrounded by the endomysium. Resident macrophages, interstitial cells, and muscle stem cell (MuSC) are localized in the myofibers. The MuSC are the muscle stem cells between the basal lamina and the sarcolemma (not indicated in the figure). Image retrieved from[24]

The myofibers are connected by the endomysium, the internal layer of connective tissue. A muscle fascicle is a bundle of skeletal muscle myofibers arranged in parallel and surrounded by the perimysium, the medium, slightly thicker layer. Likewise, the fascicle units group to form the final muscle structure that is confined by a thick collagenous external cover, the epimysium, that stabilizes the connection between the muscle, the tendon, and the bone[18–20].

Skeletal muscle has the remarkable ability to regenerate from severe consecutive injuries[19,20]. This regenerative capacity requires the activation and expansion of myogenic satellite cells, the muscle stem cells localized in the peripheral niche of stem cells beheading the basal lamina of every myofiber[11].

1.2.2. Skeletal Muscle Aging: Sarcopenia

Despite the advancements in lifespan, the health span does not increase at the same pace, reflecting an unhealthy extra years[25]. Sarcopenia is a primary cause of vulnerability in older people, resulting in increased inactivity, loss of autonomy, and increased risk factors for comorbidities and various chronic diseases[25–27]. Sarcopenia affects humans in the fourth decade of life, characterized by a loss of 30-50% of skeletal muscle mass at the age of 80[28,29].

The European Working Group on Sarcopenia in Older People defines Sarcopenia as the loss in muscle fiber quantity and muscle strength and performance, translating into diminished cross-section fiber area and a decline in the regeneration capacity after an injury induction[27]. Age-related muscle loss is a multifactorial condition that appears in older people compromising life quality and is associated with increasing risk for physical disabilities[26,30] The primary causes for muscle loss include hormone changes, decline in physical activity, insulin resistance, nutritional inadequacies, and genetic features[27]. The main cellular alterations associated with muscle aging are schematized in **Figure 3.**

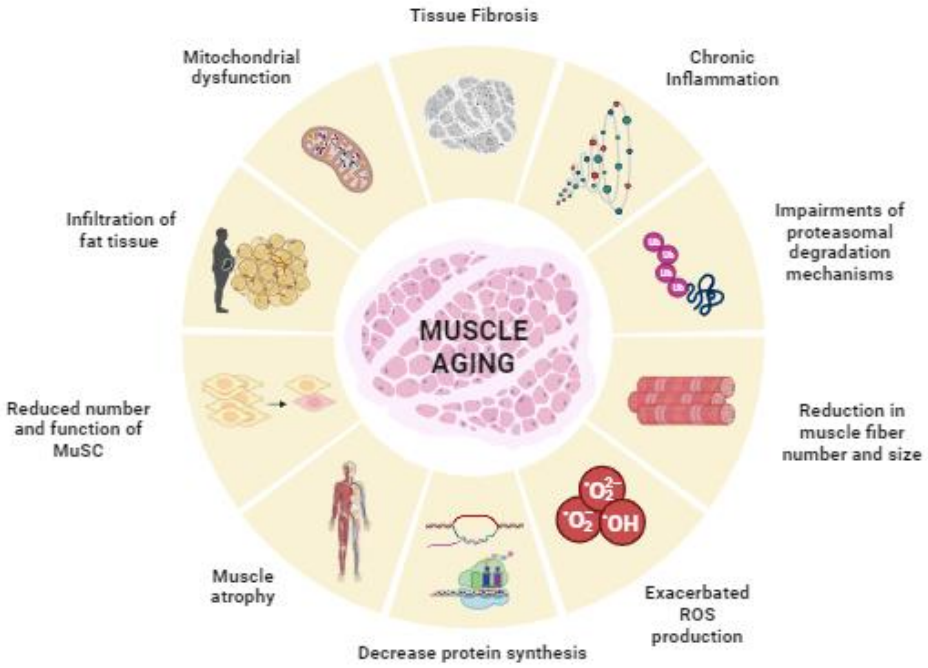

Figure 3. The main mechanisms of muscle aging. The cellular changes that contribute to muscle aging include the impairment of protein synthesis and proteasomal degradation mechanisms, leading to an accumulation of defects in the muscle. Additionally, there is exacerbated reactive oxygen species (ROS) production, chronic inflammation, and mitochondrial dysfunction at the cellular level. The skeletal muscle becomes more fibrotic, has an enhancement of fat tissue invasion, and is characterized by a decline in the number and function of MuSC, leading to regeneration failure. Muscle aging also accounts for physical disability and an increased vulnerability to several comorbidities. Image made in Biorender.

1.2.3. Skeletal Muscle Regeneration

Skeletal muscle regeneration accounts for three highly coordinated subprocesses: tissue degeneration and clearance, myogenesis, and tissue remodeling, for a successful post-injury reestablish of skeletal muscle function and structure[19,20]. It englobes sequential and overlapping phases like inflammation; clearance of damaged components; activation, proliferation, and differentiation of resident muscle stem cells, also called satellite cells, and maturation of nascent myofibers[17,31]. The success of skeletal muscle

regeneration depends on highly synchronized interactions between the satellite cells, their microenvironment, and other muscle-niche cell types, such as immune cell populations[20].

Mechanical trauma, thermal stress, myotoxic substances, ischemia, neurological impairment, and other pathogenic conditions can all cause skeletal muscle injury[31]. Administration of myotoxic agents such as cardiotoxin and notexin, chemical substances like barium chloride, and physical treatments such as freezing injury in mice skeletal muscle create various models to study muscle regeneration since they all induce injury experimentally[20,32].

After an injury, the integrity of the myofiber plasma membrane and basal lamina is compromised, generating damaged and necrotic myofibers[17,33,34]. Moreover, this necrotic environment causes an overflow of calcium from the myofibers' sarcoplasmic reticulum, promoting proteolysis and muscle atrophy and triggering skeletal muscle regeneration[31]. The tissue degradation phase begins with a proinflammatory response characterized by developing edema at the injury site with increased blood fluency, vascular permeabilization, and the recruitment of sequential immune populations to clear tissue debris[33].

The innate immune system activation occurs in the proinflammatory phase of regeneration, with the appearance of neutrophils, followed by monocytes, which may develop into macrophages in the skeletal muscle[33]. After the debris clearance, the muscle is restructured by the proliferation and differentiation of parenchymal and stromal cells, notably the satellite cells[33]. The next chapter will discuss the function of some essential immune system populations and their general role in skeletal muscle regeneration.

1.2.3.1. The Central Role of the Immune System in the Skeletal Muscle Regeneration

In an ancient timeframe, inflammation was thought to be harmful and carrying only downside effects[33]. Although chronic levels of inflammation can contribute to the development and worsening of several pathologies, research has proven the crucial and life-essential role of basal and acute inflammatory responses to damage-associated molecular patterns (DAMPs), preserving tissue homeostasis[33]. Due to its relevance, inflammation is a conserved mechanism shared by different species and accounts for an innate immune response after an injury[35,36].

In the early phases of skeletal muscle repair, myeloid cells expand in regeneration mainly due to the circulatory cell's infiltration rather than the expansion of resident leucocytes. The first myeloid cell type to arrive on the skeletal muscle is the neutrophil (**Figure 4**)[37]. By expanding their number extensively in the first hours of the regeneration process, neutrophils create a proinflammatory environment that draws monocyte influx[33,37].

Neutrophils are phagocytic cells and are characterized by expressing Ly6G surface markers[33,37]. Their first role in the injured muscle is to phagocyte damaged fibers. After performing their task, neutrophils die in the inflammation arena producing high levels of free radicals and proinflammatory cytokines. The accumulation of this inflammatory environment induces the infiltration of monocytes and, consequently, macrophages into the muscle to clear the remaining debris (**Figure 4**)[33,35,36].

Monocytes-Macrophages

Monocytes infiltration is regulated by the C-C Motif Chemokine Ligand 2 (CCL2), also called macrophage chemoattractant protein 1 (MCP-1), and the C-C Motif Chemokine Receptor 2 (CCR2) axis with some contribution of the complement protein C3a pathway[33]. Circulating monocytes present on their surface the receptor CCR2, while injured fibers, resident macrophages, and infiltrated macrophages secrete the CCL2 protein, promoting the accumulation of circulating monocytes at the injury site. This accumulation is impaired when there is a knockout of CCL2 and CCR2 genes[33,38].

After infiltrating the muscle, *in situ* monocytes rapidly transform into macrophages with a proinflammatory profile ($Ly6C^{pos}Ccr2^{pos}Cx3cr1^{low}$) to clear tissue debris from the injury site by efferocytosis. However, skeletal muscle regeneration depends upon a timely, successful phenotypic switch coordination between proinflammatory cells and anti-inflammatory (pro-repair) macrophages ($Ly6C^{neg}CCR22^{pos}CX3CR1^{high}$)[33,38]. This phenotypic switch is triggered by efferocytosis, and it promotes macrophage proliferation, the loss of the Ly6C antigen expression, and the increase of the CX3CR1cell surface marker, characteristics of the pro-repair macrophage population[33,38].

Interestingly, CCR2 knockout mice demonstrate that this macrophage transition occurs in the tissue from monocytes, and it is not a result of a secondary myeloid cell recruitment wave like the neutrophils and monocyte infiltration[39,40]. Ablation of the CCR2 gene suppressed the Ly6Cneg macrophages population in the repaired muscle, diminished the effect of Ly6Cneg monocytes in regeneration, and impaired the tracing of Ly6Cneg macrophages when Ly6C monocytes engulfed fluorescent beads, indicating that this phenotypic switch is independent of cell recruitment[36,40].

The pro-repair macrophages (Ly6Cneg) regulate skeletal muscle regeneration by coordinating the myogenesis and the angiogenesis processes simultaneously through the secretion of oncostatin M[41], among other factors. Fibrogenic conversion and fibro-adipogenic-progenitors (FAPs) expansion in muscle repair is further regulated by pro-repair macrophages that balance the release of tumor necrosis factor alpha (TNFα) and transforming growth factor beta 1 (TGF-β1) to orchestrate FAPs apoptosis and differentiation[42].

Aging accounts for defects in the transition of macrophage phenotypes, impairing muscle regeneration[43]. Despite there being no significant alterations in the proinflammatory population

(Ly6Cpos), the pro-repair macrophages (Ly6Cneg) are reduced by half in aged animals (23-25 mo), contributing to the decline of the myeloid total number of cells in the muscle at 3dpi[43].

The immune system is a central player in regulating skeletal muscle regeneration and is also affected by aging. Age-related alterations in the immune system occur in the aged skeletal muscle, in homeostasis, with detrimental consequences for MuSC activity. However, the investigation into how aging affects the myeloid response related to muscle regeneration is just beginning[36,43]

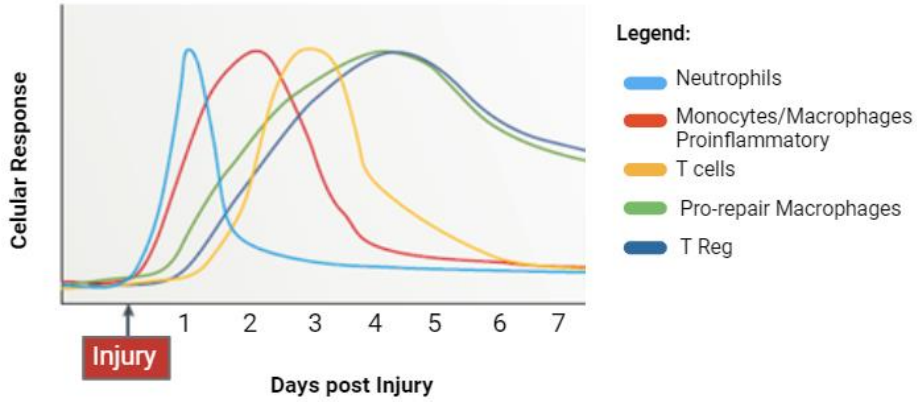

Figure 4. Inflammatory response after an Injury. Blue: Neutrophils, Red: Monocytes/Macrophages proinflammatory, Yellow: T cells, Green: Pro-repair Macrophages, Dark blue: Regulatory T Cells (T reg). After an injury, the skeletal muscle is rapidly infiltrated by time-coordinated immune populations. Image retrieved from[44].

1.3. The Adult Muscle Stem Cells

Through electron microscopy, Alexander Mauro discovered MuSCs in the early 60s[45]. Stem cells consist of undifferentiated cells located all over the body and have a potential for self-renewal and differentiation into all cell types of an organism[12,46]. The process of specialization involves multiple stages and depends on the potency degree of a cell. Hierarchy potency is indirectly proportional to the cell's differentiation degree, meaning that the ability of a specialized cell to differentiate into several types of cells is limited compared with an undifferentiated cell[12].

The MuSCs, are unipotent stem cells[11] that confer to the skeletal muscle the ability to recover from consecutive acute damages over the years. These cells fully re-establish the contractability and structure of the skeletal muscle and are gathered under the basal lamina adherently to the plasma membrane of the muscle fibers in a unique and specific niche environment[11].

MuSCs in a resting muscle are generally quiescent[11,12,46], characterized by a transitory cell cycle inhibition (Go phase) with limited metabolic activity. This dormant but active process is highly sensible

to modified signals from the niche that activate MuSCs to boost their myogenic activity in response to several mild and severe damages[11,12,46].

Through increased biosynthetic activity, activated MuSCs migrate into the injured site and re-enter the cell cycle to differentiate into myofibers or self-renew, restoring the quiescent MuSC pool[11]. This asymmetric division continuously allows future repairments of skeletal muscle while ensuring that the MuSC population remains constant[11].

1.3.1. The Myogenesis Process

MuSCs are transcriptionally defined by a family of the paired box/homeodomain transcription factors: PAX3 present in early embryogenesis and PAX7 expressed from that stage forward[11,47]. MuSC survival depends on the antiapoptotic function of PAX7; therefore, it is ubiquitously expressed between different MuSC stages[48]. Although PAX3 (a paralogue of PAX7) was also confirmed to be present in both quiescent and activated adult MuSCs, it could not compensate for PAX7's vital function in stem cells[48].

Myogenesis is the sequential differentiation cell process of MuSCs that culminates in forming muscle fibers upon an activated stem cell asymmetric cell division[11,47]. It depends on the expression of muscle regulatory transcription factors (MFRs): MYOD, MYF5, myogenin, and MRF4 are time-coordinated and characterize sequential specialized stages of MuSC during embryogenesis or upon damage[11,47]. They regulate proliferation through the cell cycle and activate sarcomeric-specific sequences in the DNA to promote differentiation by the sarcomere assembly (**Figure 5**)[11,47].

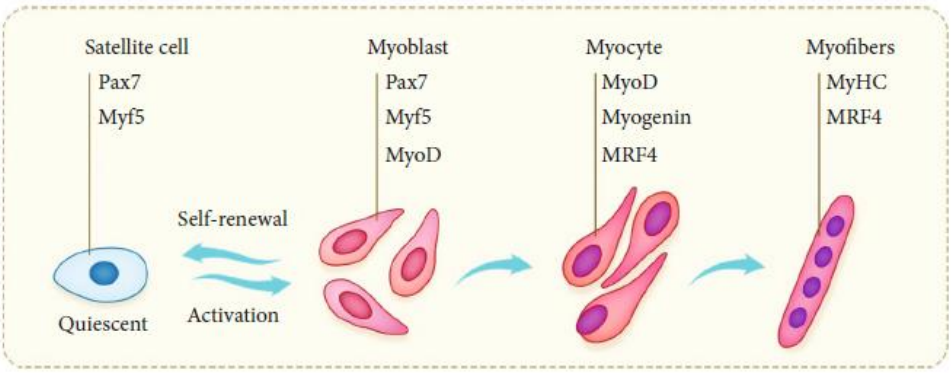

Figure 5. Differentiation course of quiescent MuSC muscle activation. A myofiber is originated from a quiescent MuSC through different timely-dependent MRFs expression factors. To respond to future regeneration demands, a small percentage of activated cells divide asymmetrically, preserving the quiescent state (self-renew ability).

In the dormant quiescent phase, MuSCs express the Pax7 and Myf5 markers[49]. Activated stem cells migrate into the injury site, increasing their expression of the MyoD transcription factor, a robust proliferative inductor factor. This myogenic differentiation factor 1 characterizes the myoblast cell setting

the myogenic lineage fate[46,50]. MyoD gathers other myogenic factors by recruiting several chromatin-modifying enzymes functioning as a genome organizer for myofiber identity[49,51].

As the myoblast diminishes the proliferative activity, differentiation befalls, accompanied by decreased Pax7 and MYF5 gene expression[12,46,49,50]. This switch coincides with the MyoD induction of Myogenin expression. This results in a progressive manifestation of the MRF-4 gene allowing the creation of multinucleated fibers muscle cells. Additionally, MRF-4 continues to be expressed at high levels in mature muscle myocytes and induces the appearance of other late muscle differentiation genes, like MyHC, for myocytes fusion into a myofiber completing the myogenesis process[50].

Although MFRs are crucial for myogenesis, the skeletal muscle regeneration process is facilitated and optimized by proteins from the extracellular matrix (ECM)[52] and the adipose tissue[53]. In vitro, laminin, an ECM protein, is at the basal layer of the satellite cell niche and allows more robust proliferation and differentiation capabilities of MuSCs. Genetic ablation of laminin impaired MuSCs' self-renewal ability, compromising sustainable long-term regeneration[52].

1.3.2. Muscle Stem Cell Markers

MuSCs can be identified based on their spatial site in the muscle: externally of the plasma membrane and internally of the basal lamina, and their shape: small cells with a prominent nucleus and few intracellular components supporting the quiescent state in the majority of the time[11]. However, for fluorescence microscopy recognition, distinctive MuSC biomarkers are preferable[12,46,47].

Although there are many MuSC markers to identify this population, due to the heterogenicity of this population is not probable that a single cell embarrasses all of those markers simultaneously[11,12,46]. Therefore, the MuSC population is recognized by identifying positive and negative markers[12]. In this project, MuSC were discriminated by using the following strategy $CD45^{neg}CD31^{neg}Sca\text{-}1^{neg}\alpha7int^{pos}$ (see the gating strategy in Methods Section)

Hematopoietic[54], endothelial[55], and fibro-adipogenic progenitor[56] cells are characterized by being respectively CD45, CD31 and Sca-1 positive populations. The α7 integrin is a laminin receptor on the surface of MuSC and myofibers that facilitates the migration and proliferation processes in myoblast development[57].

1.3.3. Heterogenicity of MuSCs

Oppositely to what was initially thought, MuSCs are a heterogenic population preserved over the years, providing an adaptability advantage facing challenging environments[11,12,46].

Different subpopulations of MuSCs are preserved in homeostatic adult muscles[11]. After an injury, however, multicolor lineage tracing experiments showed that symmetric cell divisions lead the MuSCs to lose their heterogenic identity and reduce their subpopulational clonal diversity[11].

Gene expression, epigenetic marks, cell surface markers, and distinct functionality (for example, division rates, self-renewal capacity, and stress resistance) categorize different subpopulations of MuSCs[11]. However, due to the extensive information on this topic[11], this work will focus only on the heterogenicity of Sca-1 in MuSC.

A small population of MuSC positive for both Sca-1 and ABCG2 surface markers (distinctive from the majority of MuSC Sca-1neg ABCG2neg) exists in the muscle, and despite being able to proliferate with a reduced contribution in myofiber production, preferably return to dormancy in the MuSC niche[12].

MuSC can be both negative or positive to Sca-1 marker[58]. Most MuSCs in the skeletal muscle are Sca-1neg, and the newly formed myoblasts are heterogeneous for Sca-1 expression[58]. A small positive Sca-1 population was also detected; however, it had a slower dividing profile and did not form myotubes as instantly as the negative population[58]. The importance of this population remains unknown, but it is likely to restrict the proliferating and dividing ability of MuSC, conserving their replicative capacity[58].

In sca-1 null mice, myofiber size increased in young animals and decreased in aged ones[58]. Thus, it demonstrated that sca-1 modulates myoblast behavior and is influenced by the microenvironment[58,59].

1.3.4. MuSC Aging: Impact on Skeletal Muscle Regeneration

Although the skeletal muscle can perform consecutive regenerations over time, this condition is impaired in aging mainly due to the loss of MuSC number and function[60,61]. MuSC aging contributes to decreasing myofibers' cross-section area[11], and it is associated with intramuscular fat deposition, fibrosis, and chronic inflammation, impairing skeletal muscle regeneration. Regarding fibrosis, a recent study demonstrated that the myogenic progenitors interact with the extracellular matrix composition, modifying it in aging to induce environmental fibrosis[62]. Notably, declining aged muscle mass is linked to the reduction of MuSCs since the myofiber size and composition are dependent on that loss in old mice with physical activity[63].

MuSC aging is influenced by numerous interdependent cell-intrinsic and cell-extrinsic mechanisms, which frequently interact, affecting the regulation of stem cell function[47]

1.3.4.1. Aged MuSC's intrinsic changes

The Janus kinase/signal transducers and activators of the transcription (JAK/STAT) pathway is upregulated in aging[64]. MuSCs became pathologically committed to differentiation, leading to the depletion of the stem cell pool and provoking muscular dystrophy through the deregulation of MuSC

homeostasis[64]. Inhibition of the JAK/STAT pathway resulted in a significant augmented of the MuSC number, the asymmetric division potential restoring the stem cell pool, and improved skeletal muscle regeneration[64].

The quiescent mode of the MuSC is vital to enduring long-term skeletal muscle regeneration. The reversible phenotype of quiescent MuSC is lost during aging since aged MuSC enters an irreversible state through weak repression of senescence pathways like p16(INK4a)[65]. By inhibiting the cell cycle regulator p16(INK4a), skeletal muscle function improved overall[65].

Furthermore, aged MuSC self-renewal ability is mainly downregulated[60,61]. However, a small resistance population of aged MuSC keeps their usual ability to do it successfully[66].

Besides JAK-STAT, with aging, there is dysregulation of other signaling pathways, like canonical Wnt and Notch signaling, that decline the MuSC functionality[61]. Moreover, aged MuSCs also incorporate changes in the metabolism and proteases, autophagy, epigenetic patterns, and cytokine production[60,61]. Although aged intrinsic alterations are crucial in determining the MuSC fate, niche environment factors also significantly impact skeletal muscle and MuSCs[60,61].

1.3.4.2. Aged MuSC niche modifications

Experiments with heterochronic parabiosis provided the primary proof for systemic variables altering MuSC function[67]. When aged mice were exposed to a more youthful systemic environment, skeletal muscle regeneration was improved through increased MuSC proliferation and differentiation and decreased fibrosis. In vitro experiments corroborated this study, implying that serum factors modulate MuSC proliferation and cell fate.

Aged MuSCs are influenced by factors that reach skeletal muscle via the bloodstream and factors secreted into the MuSC niche environment directly.

Stem cell niche strongly impacts the number and fitness of the MuSC. FAPs (Fibro-Adipogenic-Progenitors), macrophages, and other cells secrete molecules and cytokines that change the ECM and the MuSC niche composition.

The immune system is one of the most fundamental contributors to the regenerative cell niche, and age-related modifications in the immune system have negatively impacted the MuSC function[68]. Old mice have been observed to be responsive to muscle injury with a delayed kinetics transition and altered macrophage inflammatory/anti-inflammatory profiles, which affect their interaction with MuSC[68].

Old bone marrow-derived macrophages (old-BMDMs), which have been developed from bone marrow cells (BMCs) of aged mice, caused significantly less proliferation in myoblasts than myoblasts treated with youthful BMDM. Studies show that with aging, macrophages change their gene expression pattern

and can directly influence the proliferation and differentiation of MuSC cells Some examples are the decline in MyoD, GDF3, and Klotho and the increase in gene expression in the osteopontin[69].

IFN-responsive macrophages, also known as IFNRMs, are a new subgroup of macrophages that interact with MuSC in muscle through the particular expression of interferon (IFN) responsive genes[70]. IFNRMs generate C-X-C motif chemokine ligand 10 (CXCL10), which, through its receptor C-X-C motif chemokine receptor 3 (CXCR3), promotes MuSC proliferation and differentiation. Aging declines the number of IFNRMs, negatively affecting the MuSC cell. Recombinant CXCL10 therapy can restore MuSC function and skeletal muscle regeneration in old mice because the number of IFNRMs declines with age.

Additionally, a zebrafish study revealed that a distinct subset of macrophages was crucial for MuSC proliferation and muscle regeneration[71], highlighting a strict relation between macrophages and MuSC function in regeneration.

Furthermore, aged FAPS presented decreased interleukin 33 (IL-33) production, resulting in ineffective Treg recruitment. This aged defect affected the MuSCs, impairing skeletal muscle regeneration[72].

Concluding is clear that niche interactions with MuSC are essential to sustain skeletal muscle regeneration. Aging-related niche alterations promoted by other cell types residing in the stem cell niche and those cells recruited for the skeletal muscle during an injury modulate the fitness and function of the MuSC. However, research on the consequences of age-related changes of the niche in MuSC is just starting to be understood.

1.3.4.3. MuSC Cell Fate Changes

The microenvironment in which MuSCs reside plays a significant role in regulating their behavior. Aging can lead to changes in the signals and interactions within the niche, affecting MuSCs' activation, proliferation, and differentiation (intrinsic impairments). Although the young environment promotes the MuSC quiescence, the aged stem cell niche boosts the expansion and the differentiation of the MuSC[72]. Furthermore, aging reduces MuSCs self-renewal by repressing chromatin marks of quiescent cells[11,47].

Aged MuSCs may differentiate into non-muscle lineages (such fat or fibrous tissue) instead of forming functional muscle fibers[11]. This may lead to the accumulation of non-functional tissue in aging muscles[11].

Myoblasts from 23-month-old mice expressed genes typical of functional adipocytes and retained fat[73]. This change in differentiation potential was linked to the increase of the transcription factor C/EBP, and the proportion PPAR2/PPAR1 mRNAs expression[73]. The PPAR and C/EBP transcription factors are known to block the MuSC differentiation by inhibiting the HLH family of transcription factors[73]. Theoretically, this suggests that a MuSC adipogenic differentiation could impair the myogenesis process in aging, but experimental results were not significantly different[73].

Moreover, as they start to proliferate, MuSCs from elderly mice tend to switch from a myogenic to a fibrogenic lineage, and elements in the systemic environment of the old animals mediate this switch[74]. This lineage conversion in aged mice is accompanied by activation of the canonical Wnt signaling pathway, which Wnt inhibitors can block[74]. Therefore, the Wnt signaling pathway plays a vital role in tissue-specific stem cell aging and an increase in tissue fibrosis with age[74].

To sum up, alterations in aged MuSC stimulation, expansion, and self-renewal can induce fibrogenic or adipogenic differentiation deviations in some old MuSCs' lineage fate[11]. The loss in skeletal muscle regeneration capacity with age, which is accompanied by muscular weakness, atrophy, and poorer functional recovery after injury, is caused, in part, by these collective cell fate alterations of the aged MuSC[60,61]. Developing ways to improve muscle regeneration and protect against age-related muscle loss and dysfunction requires understanding these changes[61].

To address these problems and encourage healthier aging, researchers actively look into various interventions like physical activity, dietary supplements, and regenerative medicines[61].

1.4. Interferon as an Immune System Target

The discovery of interferon emerged during viral infection studies in 1957 by Alick Isaacs and Jean Lindenmann[75]. Interferons are essential cytokines released to modulate immunity and inflammation systemically and localized. In autoimmune diseases, interferons potentiate chronic inflammation; however, more recently, interferons have been implicated in preserving tissue homeostasis integrity in normal conditions[76,77].

The type-I family clustered on chromosome 9 in humans and on chromosome 4 in mice includes 13 different subtypes of IFNα (IFNα- 1, 2, 4, 5, 6, 7, 8, 10, 13, 14, 16, 17 and 21), IFN-β, IFN-ε, IFN-κ, IFN-τ, and IFN-ω[76,77]. The type-II family, also known as IFNγ, gaggles on the 12th chromosome in humans and the 10th chromone in mice[77]. Genome analysis studies discovered more recently the third type of interferon (type-III), which is subdivided into four types: IFN-λ1, IFN-λ2, IFN-λ3, and IFN-λ4[78]. Type III is localized in chromosome 19 in humans and chromosome 7 in mice[78].

IFNα belongs to the type-I family and is produced by hematopoietic cells, particularly plasmacytoid dendritic cells. Its responsible for augmenting the production and recruitment of crucial chemokines coordinating the proinflammatory environment[79]. Regarding IFN-γ, natural killer, ILC1, and γδ T cells are innate immune producers, while CD4+ and CD8+ T cells are the adaptative immune origins of IFN-γ[77,80]. The main targets of IFN-γ acts are T cells and macrophages[77] and potentiates a pro-inflammatory environment[77,79,80].

Regarding the skeletal muscle, the interferons can have distinct functions. In the presence of type I interferon, apoptotic cell-derived autoantigens are generated, inducing autoimmunity[24]. IFN type I stimulates muscle atrophy gene expression, provoking myofiber damage, and impairs myoblast differentiation by reducing myogenin expression levels[24]. In endothelial cells, IFN type I disrupts vascular junctions by inhibiting the angiogenesis process in vitro[80]. The IFN-γ is an inflammatory cytokine that suppresses myogenesis and impairs muscle regeneration[81]. However, in a PD-1 deletion mouse model, IFNy blocked increased skeletal muscle inflammation and fibrosis, affecting muscle regeneration through declining macrophage accumulation and transition, promoting infiltrating neutrophils[82].

1.4.1. The JAK-STAT Pathway

The JAK-STAT is an evolutionarily well-preserved pathway that comprises in total four types of JAKs (JAK1, JAK2, JAK3, and TYK2) and seven types of STATs (STAT1, STAT2, STAT3, STAT4, STAT5a, STAT5b, and STAT6) in mammals[83,84]. Distinct JAK and STAT patterns of protein combinations respond to unique groups of cytokine or growth factor signals, ensuring a high degree of sensitivity with different in vivo activities[83,84]. Over 50 cytokines and growth factors, including hormones, interferons (IFN), interleukins (ILs), and colony-stimulating factors, use the JAK/STAT signaling pathway to promote downstream intracellular signals[83]. Mutations in the JAK and STAT genes have been closely associated with autoimmune and malignant diseases[83]. Therefore, inhibiting this system may be a promising treatment for various disorders[83].

The starting point for the three IFN families' pleiotropic biological activity is the binding and subsequent assembly of heterodimeric receptor complexes on the cell membrane, as exemplified in **Figure 8**. The JAKs constitutively engage the IFN receptors' intracellular domains (ICDs) through non-covalent interactions[83,84]. Phosphorylation of JAK tyrosine residues leads to the activation of the kinases and consequential STAT-pathway-specific activation[83,84]. Stimulated STATs translocate from the receptor to the cytoplasm, where they dimerize in a homozygotic or heterozygotic manner. STAT dimers migrate into the nucleus to activate transcription factors of the target genes[83,84].

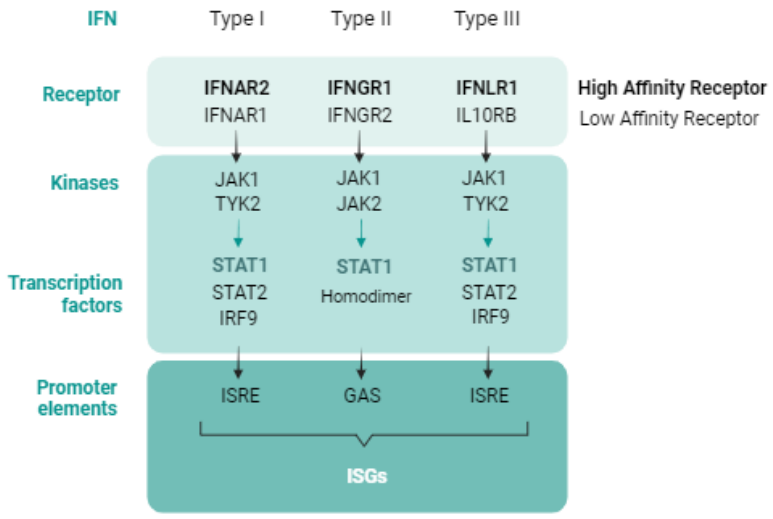

Figure 6. The three IFN pathway types. Type I binds to the IFNAR1-IFNAR2 complex, type II attaches to the IFNGR1-IFNGR2 heterodimer, and the type III IFN family connects with the IFNLR1-IL10RB receptor complex. After this initial activation, type I and III used the same intracellular domains (JAK1-TYK2), whereas type II uses JAK1 and JAK2. The high-affinity receptors IFNAR2, IFNGR1, and IFNIR1 bind to JAK1, whereas the low-affinity receptors IFNAR1 and IL10RB activate TYK2, and the IFNGR2 stimulates the JAK2. After the phosphorylation of the kinase, they activate the transcription factors, which enter the nucleus to regulate gene expression. In types I and III, a heterodimer is formed of STAT1 and STAT2 with a complement of IRF9. In contrast, type II activates homodimers of STAT1. The signaling transduction culminates in the transcription of Interferon-sensitive response element (ISRE) and interferon gamma-activated site (GAS) elements. The interferon-stimulated genes (ISGs) encode important molecules for antiviral responses, antigen presentation, autoimmunity, and inflammation. Image retrieved from[85].

1.4.1.1. JAK-STAT pathway: Myogenesis commitment, Self-Renewal symmetric proliferation and multilineage plasticity

The JAK1-STAT1-STAT3 signaling pathway prevents early differentiation, functioning as a regeneration checkpoint[86,87]. IL-6 is a cytokine that can activate the JAK1-STAT1-STAT3 pathway, inhibiting myoblast differentiation, and is produced by macrophages, neutrophils, FAP cells, and myofibers[88]. In low concentrations, IL-6-STAT3 is crucial for satellite cell proliferation[88]. However, chronic IL-6 elevated concentrations impair muscle regeneration[88].

Inhibition of JAK2 declined the levels of myogenic factors, compromising myoblast differentiation[86,89]. While JAK2-STAT2-STAT3 promotes differentiation, studies with LIF (leukemia inhibitory factor) demonstrated that the JAK2-STAT3 pathway modulates satellite cell proliferation at least partially[90]. Myoblast cells also express JAK3. Blocking the JAK3 function promoted myogenic differentiation, revealing the suppressing JAK3 function in this process[86].

Studies suggest that the activation of STAT1 by Il-6 is less pronounced than other STAT1 activating cytokines mainly because there is a formation of heterodimers STAT1/STAT3 instead of STAT1/STAT1[91] it is known that IL-6 provokes a transient activation of STAT1 kinetics[91].

Despite cell fate commitment and self-renew abilities, in prostate cancer studies, the JAK-STAT pathway's continuous activation induced a stem-like tumor phenotype by promoting multilineage plasticity, conferring tumor resistance in this clones[92]. Inhibiting this pathway represents a therapeutic solution to overpass this multilineage plasticity characteristic making the tumors more sensible to effective oncology therapies[92].

1.4.2. Interferon and JAK-STAT Pathway: The Impact of Aging

Aging and age-associated comorbidities increased susceptibility to viral infections due to IFN age secretion impairments. Administration of type I and III IFN in an early phase of viral infection can be beneficial, comparatively with delayed IFN treatments that potentiate the inflammatory environment[93]. In aged skeletal muscle, MuSC functional impairments have been linked to a decline in macrophage-specific IFN-γ response[70]. Injections of CXCL10, an end product of the IFN-γ pathway, rejuvenated the aged MuSCs function and restored muscle repair of old mice[70].

Aging is accompanied by chronic inflammatory responses due to elevated circulatory inflammatory cytokine production[2,5,8,47,70]. In aged mice, there is a shift from Type 1 (IL-2, IFN-γ) to a Type 2 (IL-4, IL-6, IL-10) cytokine response[94]; however, if that shift happens similarly in humans is still controversial[95].

High levels of proinflammatory cytokines expression characterize low-grade chronic inflammation. IL-6 is a proinflammatory cytokine that increases in aging[86,93,94], impairing muscle strength and promoting age-associated environment stress through the accumulation of senescence-associated secretory phenotypes[96].

MuSC JAK-STAT pathway is known to be significantly impacted by the aging muscle environment[20,70,96]. Overactivation of the JAK-STAT pathway in MuSCs pathologically induces myogenic commitment and culminates in regenerative insufficiency in aging[97]. Blocking of the JAK2 pharmacologically improved the symmetric growth of satellite cells in vivo, promoting the repopulation of the cells in the niche[97]. However, the role of others JAK-STAT components activated by interferon in the aged MuSC is still very little explored. The world's aging population emphasizes the need to discover therapies that boost the activity of MuSC while preserving the stem cell niche and maintaining the skeletal muscle structure and function[20,70,96].

1.5. Main Goals of the project

The goal of this project is to understand why muscle stem cells are lost under regenerative pressure in conditions of immune dysfunction, as observed in aging, and study the potential impact of interferon on MuSC behavior.

The specific aims consist of:

1) Characterize the dynamic of α7Int^{pos}Sca-1^{neg} MuSC population number and behavior (proliferation, apoptosis, cell death and senescence) in young mice where macrophages were eliminated by the administration of clodronate during the first three days of skeletal muscle regeneration,

2) Characterize the α7Int^{pos}Sca-1^{pos} MuSC population regarding number and behavior (proliferation, apoptosis, cell death and senescence) in young mice where macrophages were eliminated by the administration of clodronate during the first three days of skeletal muscle regeneration,

3) Characterize the effects of Interferon alpha and gamma on the cell fate switch of the MuSC population (α7Int^{pos}Sca-1^{neg} to α7Int^{pos}Sca-1^{pos}),

4) Characterize the pathway by which Interferon alpha causes cell fate changes in MuSCs during skeletal muscle regeneration

Materials and Methods

2. Materials and Methods

2.1. Animals

Young wild-type C57BL/6 mice with 2-6 months were used for this project. All animals were housed at the Rodent facility of Instituto de Medicina Molecular, a facility accredited by the Direção Geral da Alimentação e Veterinaria. The mice were bred in-house by crossing mice purchased from Charles River laboratories. The animals were lodged in ventilated cages on a standard 12/12 h light cycle within a specific and opportunistic pathogen-free environment. All live animal procedures were conducted according to the EU legislation and authorized by the Direção Geral da Alimentação e Veterinaria.

2.2. In vivo procedures

Animal manipulation in vivo was performed using different injection techniques to deliver substances of interest (**Figure 7**).

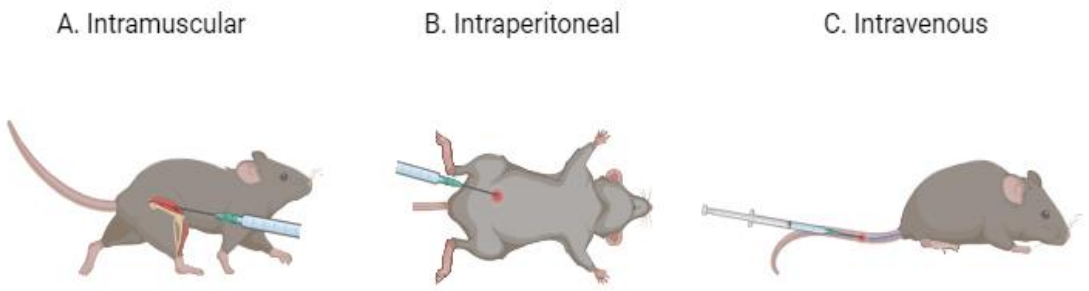

Figure 7. Types of injection techniques practiced in this project. A. Intramuscular injection for injection BaCl2, IFN's, and Poly (IC); B. Intraperitoneal injection to label cells with EdU in vivo; C. Intravenous injection for administrating clodronate liposomes.

2.2.1. Barium chloride intramuscular injection to induce injury

Barium chloride (BaCl2) was injected into the tibialis anterior or quadriceps muscle to study skeletal muscle regeneration. The BaCl2 intramuscular injection is a chemical method that provokes the muscle fiber's disintegration, triggering muscle regeneration. BaCl2 inhibits the potassium channels depolarizing the sarcolemma of the fasciculus, which leads to an overload of Ca2+, triggering myofiber disruption[31].

BaCl2 has been shown to cause total degeneration in the tibialis anterior muscle after three days, with complete regeneration observed after 14 days[18].

After being anesthetized with isoflurane, mice receive an intramuscular injection of 1.2% (w/v) of BaCl2 (Sigma-Aldrich) in saline solution to induce injury. It was administrated 40 µl of BaCl2 solution for the tibialis anterior and 50 µl for the quadriceps muscles. The **Figure 8** represents schematically the localization of the tibialis anterior and the quadricep muscle in the mice. The muscle was harvested at different time points after injury induction.

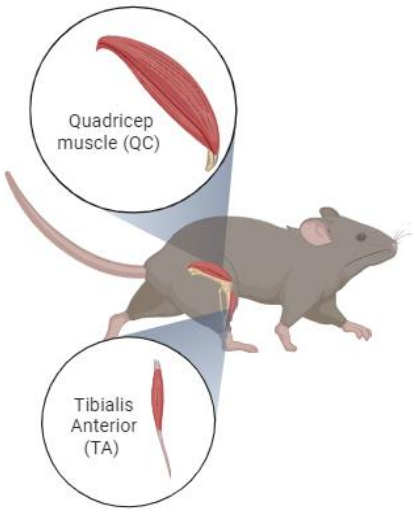

Figure 8. **Representation of mouse hindlimb: tibialis anterior muscle** (TA) localized in the inferior part of the scheme, and the quadricep muscle (QC) represented in the superior part of the figure. Single intramuscular injections of BaCl2 were given on TA or QC to induce muscle injury. Figure created with Biorender.com.

2.2.2. Intravenous injection of liposome containing clodronate

Clodronate liposome solution can be applied as a chemical strategy to eliminate macrophages, prominent immune populations recruited after an injury. The principle of this method relies on macrophages' apoptosis upon clodronate liposome phagocytosis[98]. Macrophage ablation during regeneration was applied to mimic defects in the myeloid response that happen during regeneration in aged animals[43].

Clodronate-liposomes or PBS liposomes (control group) (LIPOSOMA – Research solution SKU: CP-005-005) at 5mg/ml were injected intravenously at 100ul/10g of body weight. The liposomes were stored at 4ºC and warmed at room temperature just before use, and gently shaken to avoid liposome precipitation, ensuring a homogenous drug delivery.

The daily injections were initiated on the day before injury and lasted until the day before tissue collection (**Figure 9**).

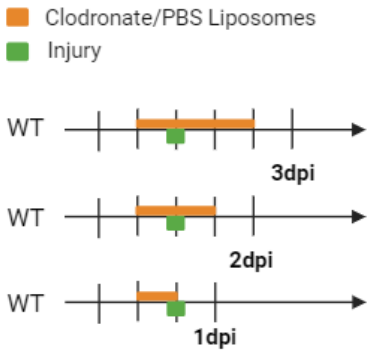

Figure 9. Experimental design of clodronate/PBS liposomes injection. Three experimental designs were made to study skeletal muscle regeneration with macrophage ablation at consecutive time points. Muscles were analyzed at 1dpi, 2dpi, and 3dpi. Figure created with Biorender.com. dpi (day post injury).

2.2.3. Intramuscular injection of Interferon alfa, gama and Poly I:C

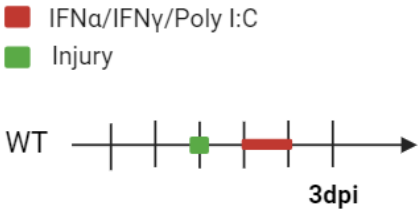

Figure 10. Experimental Design of intramuscular injections of IFNα, IFNγ and Poly IC. These compounds were administrated for two consecutive days, after performing an injury in wild-type animals. dpi (day post injury), IFNα, (interferon alpha), IFNγ (interferon gamma).

Interferon α (IFNα), interferon γ (IFNγ), and Polyinosinic–polycytidylic acid sodium salt (Poly I:C) were administrated intramuscularly in wild-type mice following the experimental design schematized in the **Figure 10**. The quantities administrated are specified in **Table 1**. For the controls the same volumes were administrated with just saline solution.

Table 1. Interferon α, interferon γ, and Polyinosinic–polycytidylic acid sodium salt Poly (IC)

Compound	Abbreviation	Source	Catalogue number	In vivo quantity/muscle
Interferon α	IFNα	Biolegend	752806	164000U/muscle
Interferon γ	IFNγ	Biolegend	575308	4000U/muscle
Polyinosinic–polycytidylic acid sodium salt Poly	Poly (IC)	Merck	MFCD00131984	20µg/muscle

2.2.4. Intraperitoneal Edu injection

EdU (5-ethynyl-2′-deoxyuridine) labelling was carried out by an intraperitoneal injection of 200 µl EdU (2.5 mg/ml) dissolved in PBS, 1-day before tissue harvesting.

2.3. Processing of skeletal muscle tissue

Mice were euthanized by CO2 narcosis followed by cervical dislocation. After that, Tibialis anterior or Quadricep muscles were harvested for two main protocols: muscle processing for flow cytometry (FC) and fluorescence activated cell sorting (FACS) or histological analysis.

2.3.1. Skeletal Muscle processing for FC and FACS

After skeletal muscle collection and weight, the muscles were broken down into small pieces mechanically, first using a sterile scissor and scalpel, and then chemically by incubating at 37 ºC for 1 h in 5 ml of Dulbecco's Modified Eagle's Medium (DMEM; Corning®) media with 1% Penicillin-Streptomycin (P/S; Gibco) containing 0.2%(w/v) of collagenase B (Roche) and Calcium dichloride (CaCl2) 0.5 mM. The mixture was filtrated using a 70 µm cell strainer and washed with DMEM media containing 10% Fetal Bovine Serum (FBS; Sigma) and 1% P/S. Two cycles of centrifugation at 670 x **g 10** min at 4 ºC were performed to extract the collagenase completely. After, cells were incubated with 1x Red Blood Cell (RBC) lysis buffer (Santa Cruz Biotechnology) for 10 min on ice protected from light (to eliminate red blood cells), and the reaction was stopped with 9 ml of DMEM with 1%P/S. Cells were centrifugated with the same parameters as mentioned before, the supernatant was removed, and the cells were resuspended in 1ml of DMEM with 10% FBS 1% P/S. For counting the number of cells, a hemacytometer was used.

2.3.2. Fluorescence-activated cell sorting (FACS) and flow cytometry analysis

Flow cytometry is a multivariable single-cell suspension analysis technology. Every particle is measured for one or more fluorescence dyes and visible light scatter: the forward direction (FSC) refers to the cell size, and the side scatter (SSC) indicates the cell surface complexity in a short period. Light scatter and fluorescence parameters are independent. Cells in a buffered salt-based solution, also called sheath fluid (FACS buffer), are pressured to pass one by one in front of the lasers. Due to hydrodynamic focusing, the heterogeneous cells injected into the sheath fluid (with higher pressure than the laminar fluid) can migrate individually through a laser beam. The detectors convert the intensity signal into an electric signal that can be analyzed in the software posteriorly (FlowJo™ v10.8 Software (BD Life Sciences)). Fluorescence-activated cell sorting (FACS) technique differs from the previous one since it isolates different cell populations for future analysis[99].

After the muscle processing protocol, single-cell suspensions were incubated with: fluorochrome-conjugated antibodies presented in **Table 2** in a density of 1x106 cells/100 µl in FACS buffer (PBS with 10% HS) for 30 min at 4ºC. The mixture was protected from the light. Then, the cells were centrifuged at 500g 5min and re-suspended in FACS buffer and filtered onto a 5 ml polystyrene Falcon tube, proceeding to FACS or FC analysis. The gating strategy used for analyzing Immune, MuSC α7Integrin^{pos}Sca-1^{neg} and α7Integrin^{pos}Sca-1^{pos} populations is shown in **Figures 11** and **12**.

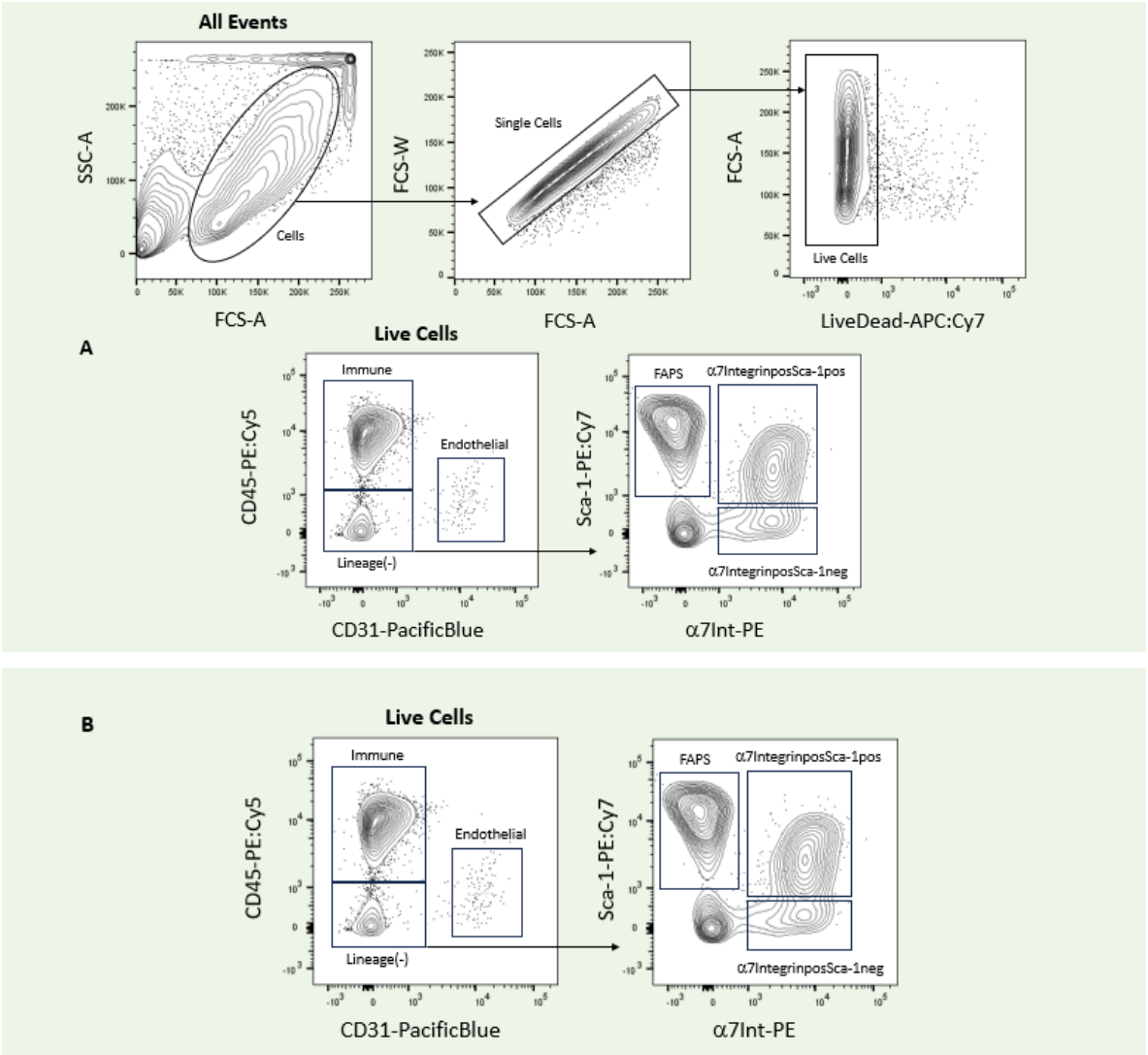

Figure 11. Gating strategy for analyzing α7Integrin^{pos}Sca-1^{neg} and α7Integrin^{pos}Sca-1^{pos} populations. All events were plotted against SSC-A/FCS-A to select the cells. After single-cell exclusion (FCS-W/FCS-A), cells that were negative to LIVE/DEAD APC:Cy7 dye were considered live cells, whereas dead cells incorporated the dye. A hematopoietic-CD45 and an endothelial-CD31 antibody were used to isolate the lineage-negative population. Then, cells were gated against Sca-1 and a7integrin markers. The α7Integrin^{pos}Sca-1^{neg} and the α7Integrin^{pos}Sca-1^{pos} populations were identified and quantified. A. Gatting strategy for analysing β-galactosidase, and Spider β-Gal activity. B. Gatting strategy for quantifying EdU proliferative activity. For Edu analysis, a different adjusted panel was used due to the incompatibility of PE-antibody staining.

Table 2. Fluorochrome conjugated antibodies panels and dyes used for flow cytometry analysis.

	Dyes	Recognized population	Source	Dilution	Filter	Host
Immune panel	PE anti-mouse F4/80	Macrophages	Biolegend (123110)	1/50	582/25	Rat
	APC anti-mouse Ly6C	Monocytes/Macrophages	eBioscience™ (17-5932-82)	1/200	660/20	Rat
	FITC anti-mouse Ly6G	Neutrophils	Biolegend (127606)	1/400	530/30	Rat
	APC-eFlour®780 anti-mouse CD11b	Myeloid lineage cells	eBioscience™ (47-0112-82)	1/200	780/60	Rat
MuSC α7Integrin^{pos} Sca-1^{neg} and α7Integrin^{pos} Sca-1^{pos} Panel I	Alexa Flour 488 anti-mouse CD31	Endothelial cells	Biolegend (102513)	1/50	530/30	Rat
	PE-Cy5 anti-mouse CD45	Hematopoietic cells	Biolegend (103109)	1/100	670/30	Rat
	PE-Cy7 anti-mouse Sca-1	Mesenchymal stem cells	Biolegend (108113)	1/100	780/60	Rat
	PE anti-mouse a7integrin	Satellite cells	Miltenyibiotec (130-120-812)	1/40	582/25	mouse IgG1κ
MuSC α7Integrin^{pos} Sca-1^{neg} and α7Integrin^{pos} Sca-1^{pos} Panel II	Pacific Blue anti-mouse CD31	Endothelial cells	Biolegend (102421)	1/50	450/50	mouse IgG1κ
	BV605 anti-mouse CD45	Hematopoietic cells	Biolegend (103139)	1/100	610/20	Rat
	V-500 anti-mouse Sca-1	Mesenchymal stem cells	BD Horizon™ (AB_10584334)	1/250	525/50	Rat
	APC anti-mouse a7integrin	Satellite cells	Miltenyibiotec 130-120-812	1/40	660/20	mouse IgG1κ
Proliferation assay	EDU	Proliferating cells	BaseClick (BCK-TCell-FC488_48)	Click Reaction	530/30	-
Apoptosis assay	Apopxin Green	Apoptotic cells	Abcam (ab176749)	1/100	530/30	-
Senescence assay	Spider-bGal	Senescent cells	Dojindo (1824699-57-1)	1/500	530/30	-
Other cell death assay	LIVE/DEAD™ Fixablenear-IR Dead Cell Stain	Dead cells	Invitrogen (L34975A)	1/1000	780/60	-

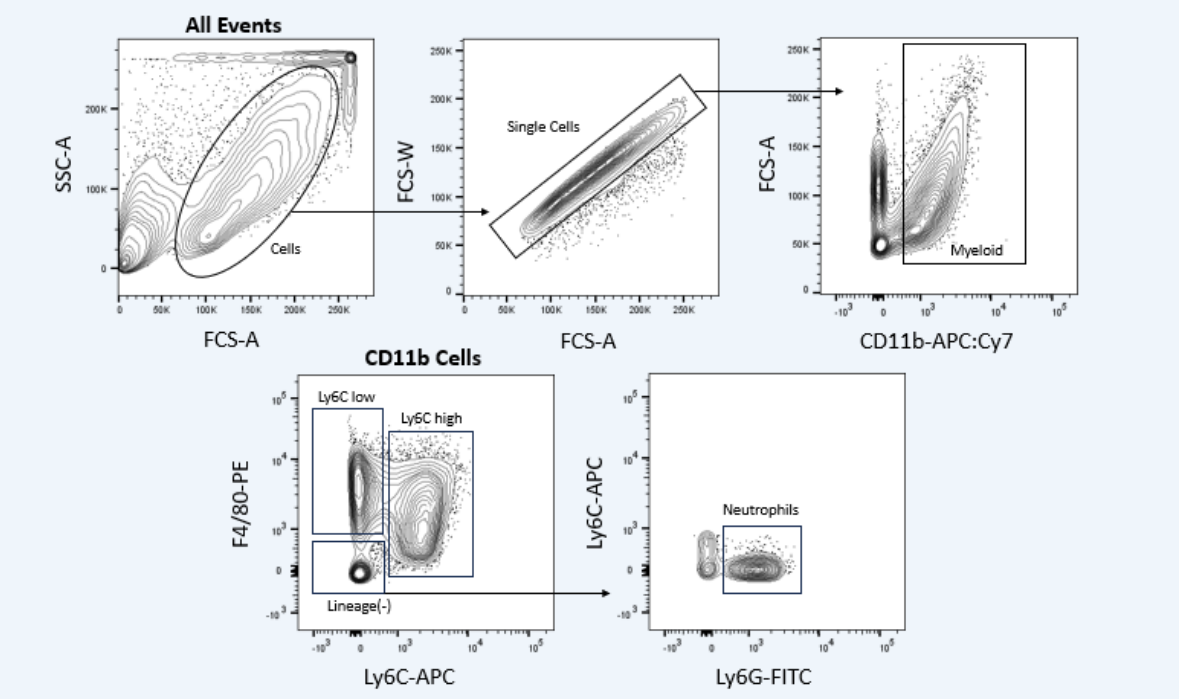

Figure 12. Immune population gating strategy. After isolating the single cells, CD11b-positive cells were selected. The myeloid population (CD11b) was divided in Ly6C low (pro-repair macrophages) and Ly6C high (proinflammatory macrophages). From the F4/80 negative population, it was also possible to isolate the neutrophils (Ly6Gpos).

I. Cell death Analysis

Cell death was measured by two methods. Apoptosis was quantified through Apopxin Green staining protocol. However, within the bulk of dead cells subjacent in every analysis, the percentage of dead MuSC α7Integrin^{pos}Sca-1^{neg} and α7Integrin^{pos}Sca-1^{pos} was measured.

a) Apoptosis analysis: Apopxin Green

Apopxin detects cell apoptosis by measuring phosphatidylserine (PS) relocation. PS travels to the plasma membrane's external layer during apoptosis[100]. Apoptosis was assessed by staining the cells with Apopxin Green solution (Abcam - ab176749).

After incubating the cells with the specific fluorochrome-conjugated antibody panels, cells were resuspended in the kit buffer with Apopxin Green indicator at 1:100 and incubated at room temperature for 45 minutes. For the FMO control, Apopxin Green dye was not added to the kit buffer (**Figure 13**).

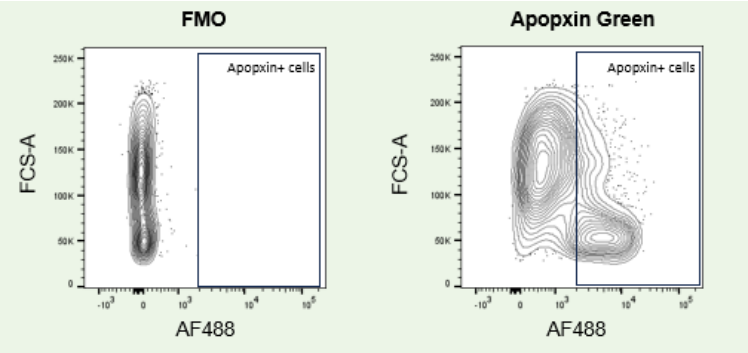

Figure 13. Apopxin Green Gating Strategy. Apopxin Green was conjugated with the AF488 fluorochrome. For every apopxin green analysis the FMO was performed. Both graphics presented were gated from the MuSC population. Apoptosis activity was measured for α7Integrin^{pos}Sca-1^{neg} and α7Integrin^{pos}Sca-1^{pos} populations.

b) Cell death analysis

The LIVE/DEAD Fixable Near-IR Dead Cell dye belongs to the family of the Amine-reactive dye and can determine the viability of a cell[101]. The dye covalently binds to free cytoplasmatic amines[101]. Dead cells have a compromised cell membrane; therefore, the dye will easily assess the free amines. Live cells exclude these dyes because their cell membranes are unbroken, and free dye is cleaned[101].

This is an irreversible reaction, therefore, even cells after fixation are permeabilized, the dye will still be bound to the free amines of the dead cells (EdU protocol)[101]. The gatting strategy for the cell death analysis is described in the **Figure 14.**

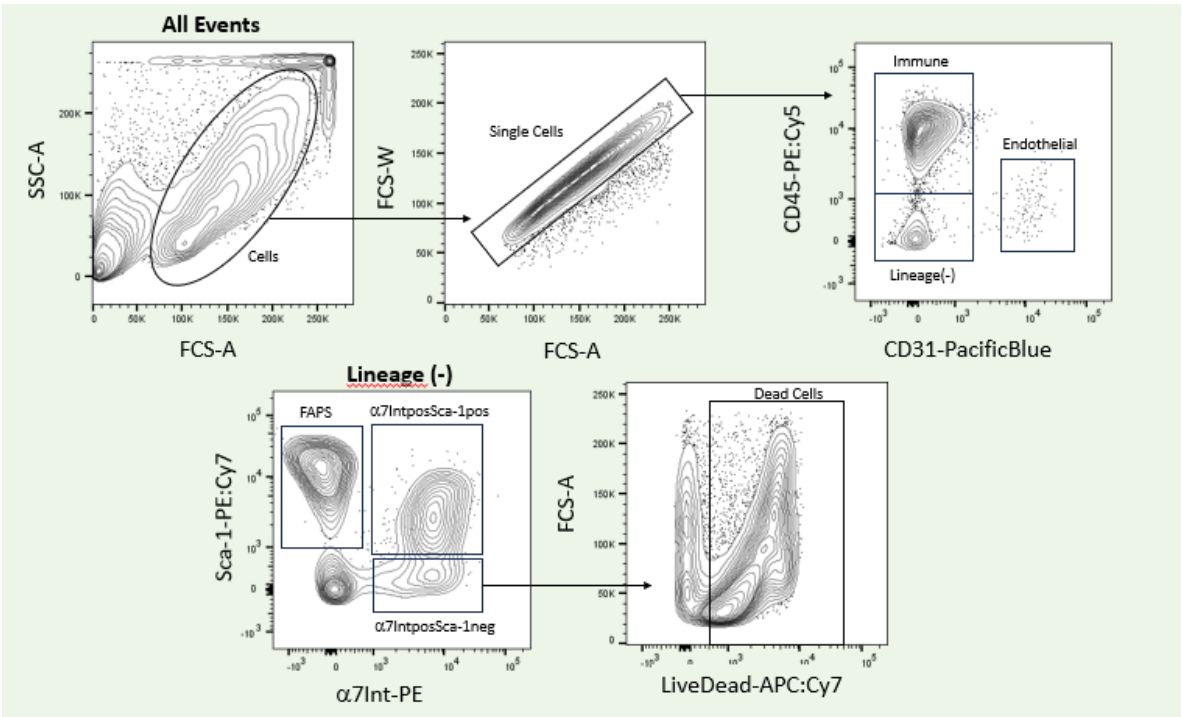

Figure 14. Gating Strategy for dead cells. The gating strategy is similar to the gating strategy mentioned in the Figure 5 with the exception that the “Live cells” discrimination is skipped. In the final of the gating strategy after

obtaining the α7Integrin^{pos}Sca-1^{neg} and the α7Integrin^{pos}Sca-1^{pos} the "Dead cells" were identified by being positive for the LiveDead-APC:Cy7. Cell death was measured for α7Integrin^{pos}Sca-1^{neg} and α7Integrin^{pos}Sca-1^{pos} populations.

II. β-galactosidase analysis

Senescent cells express high levels of β-galactosidase, a lysosomal hydrolase that cleaves terminal β-D-galactose residues[102]. SPiDER-βGal is a highly permeable probe that can migrate into the intracellular space of the cell. When SPiDER-βGal binds to the enzyme, there is a formation of a fluorescent compound that is retained in the cell[103].

Spider staining was performed during the muscle processing protocol, right after muscle digestion for 1h at 37ºC. Cells were resuspended in 1ml of DMEM with 10% FBS 1% P/S, supplemented with 2 µl of SPIDER b GaL (Dojindo - 1824699-57-1) and incubated at 37ºC for 15min. After centrifugation at 500g for 5 min, the pellet was resuspended with 5 ml DMEM 10% FBS 1% P/S, and cells undertook another centrifugation at 670g for 10 min. After that, the procedure continues as described in the "Skeletal Muscle processing for FC and FACS".

The fluorescence minus one (FMO), a negative control, was used to setup the signal threshold (**Figure 15**).

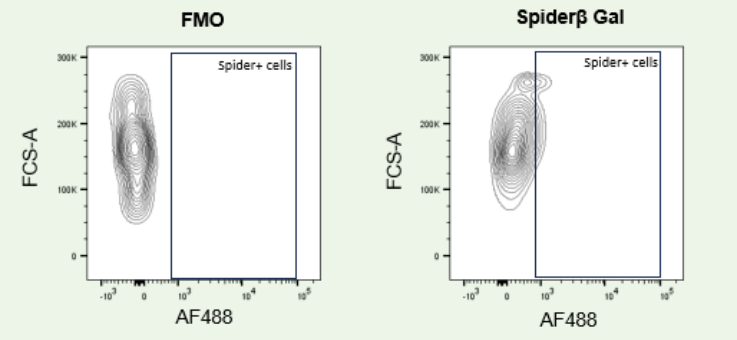

Figure 15. SPiDER-βGal Gating Strategy. SPiDER-βGal was conjugated with the AF488 fluorochrome. For every SPiDER-βGal analysis the FMO was performed to define the accurate threshold. Both graphs presented were gated from the MuSC population. Senescence activity was measured for α7Integrin^{pos}Sca-1^{neg} and α7Integrin^{pos}Sca-1^{pos}.

III. Proliferation analysis: EdU stimulation

EdU (5-ethynyl-2'-deoxyuridine) is a thymidine nucleoside analog incorporated into DNA during DNA synthesis. Unlike BrdU assays, the EdU, instead of using antibodies to detect the integrated nucleoside, employs a "click chemistry" method and therefore doesn't require DNA denaturation[104,105]. Cell proliferation was determined by EdU detection (ClickTech EdU T Cell Proliferation Kit 488 for Flow Cytometry).

After incubating the cells with the specific fluorochrome-conjugated antibody panels, cells were fixed using fixation buffer (eBioscience, 00-8222-49) 1:1 in PBS containing 5% HS. Two washing cycles of centrifugation (500g 5min at 4ºC) were performed, and cells were permeabilized in 100 µl of

permeabilization buffer (eBioscience, 00-8333) diluted 1:10 in distilled water, and incubated for 30 min, light-protected, in a cocktail reaction as instructed in the kit protocol at room temperature.

Cells were washed with 500 µl of permeabilization buffer and resuspended in PBS containing 5% HS. The fluorescence minus one (FMO) control for EdU detection was obtained, excluding the dye 6-FAM-aside from the cocktail reaction. Cells were immediately analyzed by flow cytometry (**Figure 16**).

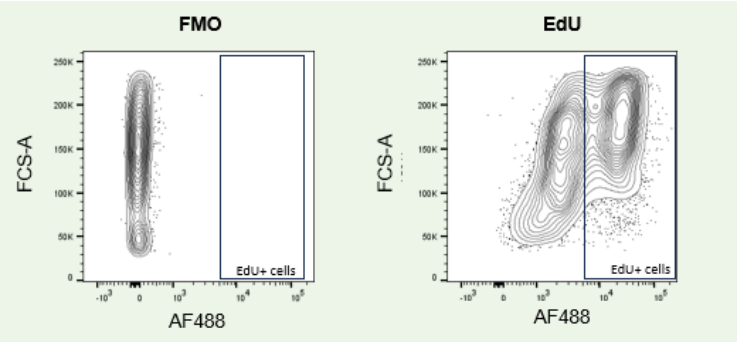

Figure 16. EdU Gating Strategy. EdU was conjugated with the AF488 fluorochrome. For every EdU analysis the FMO was performed to define the accurate threshold. Both graphs presented were gated from the MuSC population. Proliferative activity was measured for α7Integrin^{pos}Sca-1^{neg} and α7Integrin^{pos}Sca-1.

2.3.3. Collection of the muscle for histology

For histology analysis, the skeletal muscles were embedded in gum tragacanth and placed on a cardboard piece with the distal part buried in the gum and the proximal side facing up, meaning that the primary muscle sections to be cut are not surrounded by gum.

After the correct position of the muscle in the gum, the muscle was submerged in isopentane cooled in liquid nitrogen for 17s, and stored at -80 ºC, until cryosection.

2.3.3.1. Cryosectioning of muscle tissue

The frozen embedded tissue for histology analysis was cryosectioned on a cryostat (LEICA CM 3050S), and collected on microscope slides (Superfrost® Plus, Thermo Scientific).

The stored muscles were mounted on metallic structures in the cryostat and frozen for 20 min before the cut. The cryostat is at -26ºC, and the object temperature is at -25 °C; this allows the knife to be colder than the positioned muscle and make a more precise cut. The sections were collected with a thickness of 10 µm, onto slides at room temperature. Afterward, the muscle sections were at room temperature (RT) for 30 min and thoroughly dried before being stored at -80°C.

2.3.3.2. Hemotoxylin and Eosin staining

Hemotoxylin and Eosin (H&E) is a morphologic staining technique highlighting myofiber's cross-section area, degenerated, old, and regenerated myofibers, and inflammatory cells. While Harris hematoxylin (Bio-Optica) solution stains nuclei in blue, Eosin Y (Sigma- Aldrich) stains cytoplasm in red-pink color.

Skeletal muscle cryosections harvested in slides were dried at room temperature for 10 min and were hydrated in distilled water for 5min. The tissue was submerged in Harris Hematoxylin (Bio-Optica) solution for 3min and washed in running water for 5min. The slides were dipped once in 70% ethanol and four times in Eosin Y (Sigma- Aldrich) solution. Dehydration was accomplished by immersing the samples for 30 seconds in progressive ethanol-concentrated solutions of 70%, 95%, and 100% (twice). Finally, the tissue was incubated in Xylene (Leica) for a minimum of 10min and mounted with Micromount Mounting Medium (Leica) using microscope cover glass No. 1.5H (Marienfeld).

The images from H&E staining sections were acquired using a digital slide scanner (NanoZoomer SQ, HAMAMATSU), with an objective of 20X magnification.

The new myofibers were manually characterized in terms of cross-sectional area (CSA) and number to evaluate the effectiveness of muscle structure regeneration through the public domain image analysis software ImageJ.

2.4. In vitro procedures

In vitro studies were performed in immortalized myoblast C2C12 mouse cell line. Cells were cultured and kept at 37°C, 5% CO2 in Dulbecco's modified eagle medium (DMEM) with 10% fetal bovine serum and 1% penicillin-streptomycin.

2.4.1. C2C12 passages

Myoblasts were seeded on a P100 plates (Thermo Fisher Scientific) for cell line maintenance. When the myoblasts reached 80% confluence, the cells were tripsinized (Grisp, GTC02) and plated in another P100 plate in a 1:20 dillution (**Figure 17**) with replaced DMEM media.

All the cell experiments were performed in a humidified environment at 37ºC and 5% CO2.

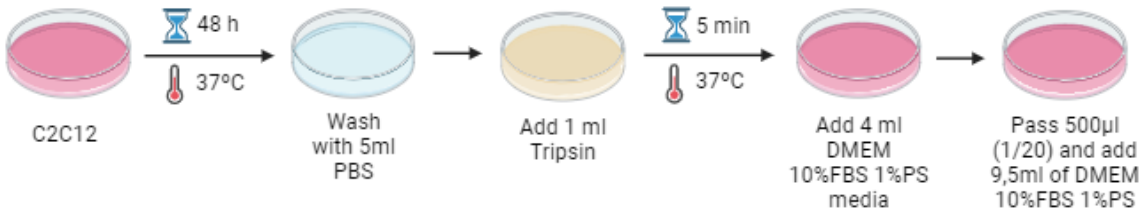

Figure 17. C2C12 passages every 48 h. After the 48h, C2C12 culture was washed with 5ml of phosphate-buffered saline (PBS). 1 ml of tripsin was added to the C2C12 to detach the cells from the plate and after 5 min at 37ºC 4ml of DMEM media were added into the solution to deactivate the trypsin effect. Cells were collected to a 1,5ml falcon and C2C12 were seeded again in a proportion of 1:**2**0 with DMEM.

2.4.2. Stimulation with IFNα, IFNγ, Poly (I:C), and Ruxolitinib (Rux)

To test whether Interferon alpha, Interferon gamma and Poly I:C promoted a direct cell fate switch in the myoblasts those compounds were experimentally administrated in vitro in C2C12 cells. Ruxolitinib (Rux) is an inhibitor of the JAK-STAT pathway since it bloks the JAK1 and JAK2 kinases[83]. It was administrated in C2C12 in conjugation with the Interferon alpha to understand if the cell fate which promoted by interferon alpha was dependent of the JAK-STAT pathway.

C2C12 cells were cultured in a 6-well plate. In each well, 15 000 C2C12 were plated in 2ml of DMEM 10%FBS 1%P/S. For stimulation, C2C12 cells were cultured in fresh 1 ml of DMEM 10%FBS 1%P/S. In the control condition, no supplementation was added. In the stimulation conditions the media was supplemented with 3270units of IFNα (0,327µg/ml), 1000 units of IFNγ (0,1µg/ml), 2µg of Poly (I:C), and 0,1µg of Rux were separately administrated. In the last well, IFNα and Rux administration was combined, with the previously established concentration values. Duplicates were done in every stimulation experiment, and the experiment was repeated until each condition reached an n=4. The administration scheme is in **Table 3**.

Table 3. 6-well plate conditions scheme for stimulation.

6-well plate				6-well plate		
Control	IFNα	IFNγ		Poly (I:C)	Rux	IFNα + Rux
Control	IFNα	IFNγ		Poly (I:C)	Rux	IFNα + Rux

Twenty-four hours after stimulation, cells were collected with 1ml of Trizol and were stored at -20ºC (**Figure 18**).

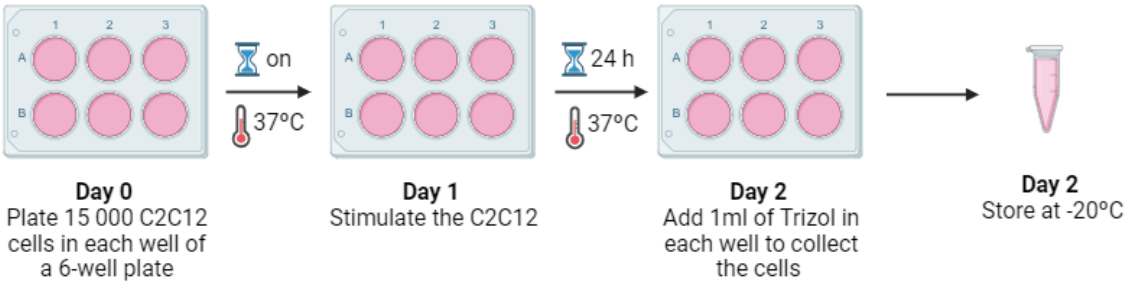

Figure 18. C2C12 cells stimulation timeline. on (overnight).

2.4.3. Proliferation assay

Cell proliferation was determined by EdU detection using an EdU-Click 488 kit. For that 15 000 C2C12 were plated in 6-well plates with 2ml of DMEM 10%FBS 1%P/S. The stimulated conditions are described in **Table 4**. It was administrated 2,5µg of EdU in each well and the EdU labeling was done 1 hour before the collection of cells (**Figure 19**), and after the fixation step, the EdU detection was done exactly as described above in the "***In vivo* section"**.

Table 4. 6 well conditions scheme for the proliferation assay. The EdU was applied in every well including, the FMO. The EdU detection step is done exactly the same way as described for the in vivo procedures.

6-well plate				6-well plate		
Control	IFNα	IFNγ		FMO	-	-
Control	IFNα	IFNγ		-	-	-

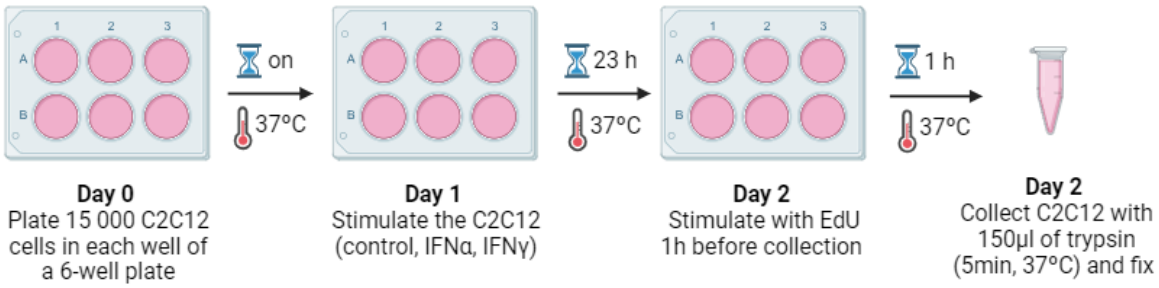

Figure 19. C2C12 proliferation assay in vitro. C2C12 were stimulated with IFNα, IFNγ or nothing (control). At the 23rd hour of stimulation, the medium was replaced in all wells including the FMO and it was added the EdU in each well with 1ml of DMEM 10%FBS 1%P/S. on (overnight).

2.5. RNA extraction and quantification

To determinate the Sca-1 gene expression from C2C12, a sequential of steps were performed culminating in the RTqPCR (**Figure 20**). The RNA extraction protocol used was the trizol method describe in the following paragraph.

2.5.1. Method: TRIZOL

Cells were resuspended in 1 ml of Trizol (Ambion 15596026), and the solution was homogenized by pipetting up and down several times. The solution was then stored at -80ºC. For the RNA isolation protocol, the samples were thawed to room temperature and 200 µl of chloroform (Merk, MFCD00000826) was added to the 1ml Trizol sample and mixed well. After a brief incubation (3 min) and centrifugation (15 min at 12000g at 4ºC), the solution was divided into two distinct phases. The superior white aqueous phase containing RNA was transferred into a new tube and incubated with 500 µl of isopropanol (Life Science, 67-63-0) for 10min. After centrifugation of 10min at 12000g at 4ºC, the supernatant was discarded, and the pellet was resuspended in 1 ml of 75% of ethanol. The mixture was vortexed briefly, re-centrifugated at 5min 12000g at 4ºC, the supernatant was aspirated, and the RNA was let dry for 10 min. After resuspension in 20 µl of RNases-free water, the mixture was incubated at 55ºC for 5 min in the heat block and stored at -80 until analysis.

2.6. RNA quantification

The extracted RNA concentration was determined using the spectrophotometer NanoDrop2000 (Thermo Fisher), and purity was analyzed using the ratios between 260/280 and 260/230 absorbances. The RNA samples were long-term stored at -80ºC.

2.7. Complementary DNA synthesis

For performing an RT-qPCR, it was nessecarly first to obtain complementary DNA (cDNA) from RNA. For converting RNA into cDNA, it was used the iScript cDNA Synthesis kit (Bio-rad). Per sample, it was used 5 µl of iScript mixture containing 4 µl of iScript Reaction Mix and 1 µl of iScript Reverse Transcriptase. 5 µl of iScript Mixture was added to 15 µl of RNA samples containing 1000ng of RNA in Nuclease Free water. After preparing the samples, they were placed in the thermocycler (C1000 Touch PCR thermal, BIO-RAD). The first cycle of the program was the priming (5 min at 25ºC), followed by reverse transcriptase activity (20 min at 46ºC) and inactivation (1 min, 95ºC). The cDNA samples stayed quickly at hold phase (4ºC) and were stored at -20ºC until RT-qPCR analysis.

2.8. Real-Time quantitative PCR

For measuring the gene expression by RT-qPCR, a 384-well PCR plate was used where each well had a correspondent primer and sample. For the reaction to occur, it was added in each well 5 µl of Syber Green MASTER MIX (Powerup SYBR Green MASTER MIX, Applied Biosystems), 3 µl of RNase-free-water, 1 µl of the desired primer mix (to detect Sca-1 expression and beta-actin expression), and 1 µl of the cDNA sample obtained previous. After a brief centrifugation at 1200 rpm for 1 min, the PCR reaction occurred in ViiA 7 Real-Time PCR System (Thermofisher Scientific), using the instrument's standard ramp speed (1.6 ºC/s) and with the amplification program described in **Table 5**.

Cycle threshold (Ct) is the number of cycles required for the fluorescent signal to exceed a background threshold value. The Sca-1 Ct value for each condition was subtracted by the β-actin Ct value. The β-actin is a housekeeping gene, and the Ct values were used to normalize the Ct value of the gene of interest (Sca-1). After, each value was subtracted by the controls media and the method $2^{-\Delta\Delta Ct}$[106] was applied to determine the relative expression of Sca-1 in each condition. Information regarding the Sca-1 and β-actin primers in in the **Table 6.**

Normalizing the results allowed comparation of the results between conditions and experiments.

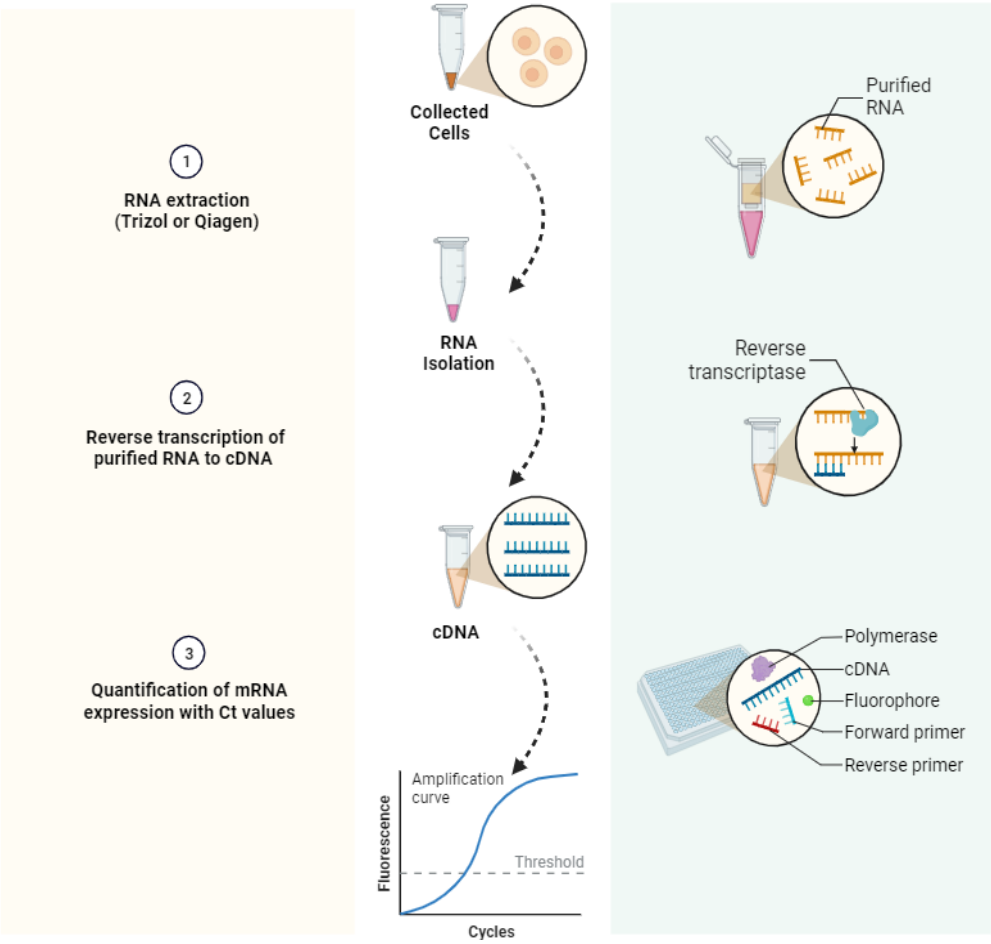

Figure 20. From cell suspension to real-time quantitate PCR analysis. The first step is to extract RNA from cells using the Trizol or Qiagen protocol. Afterward, purified RNA is converted into cDNA sequences with the addition of reverse transcriptase. Finally, mRNA is quantified by measuring the expression of Ct values.

Table 5. qPCR reaction standard program

RT-qPCR program			
	Temperature ºC	Time	Number of cycles
Hold Stage	50	2 min	1
	95	10 min	
PCR Stage	95	15 s	40
	60	1 min	

Table 6. SCA-1 and beta-actin forward and reverse primer sequences

Gene	*Spicie*	*Forward sequence*	*Reverse Sequence*
SCA-1	*mouse*	AGAAAGAGCTCAGGGACTG	TATTAGGAGGGCAGATGGG
β-actin	*mouse*	GCTCTGGCTCCTAGCACCAT	GCCACCGATCCACACAGAGT

2.9. GeneOntology (GO) Analysis

Gene ontology analysis of biological processes significantly enriched in the dataset of genes upregulated (fold change>5) in α7Integrin^{pos}Sca-1^{pos} vs α7Integrin^{pos}Sca-1^{neg} cells, isolated by FACS from mice at 3dpi. α7integrin^{pos}SCA-1^{pos} cells were isolated from clodronate-treated mice and α7Integrin^{pos}Sca-1^{neg} were isolated from control mice treated with PBS-liposomes. Cells were isolated from Pax7-TdTomato mice, which allows for lineage tracing of each population from "true" Pax7^{pos} MuSCs, identified by the expression of TdTomato protein. The Novogene team was responsible for Illumina library preparation (polyA enrichment) and sequencing using a NovaSeq instrument to generate 150-bp paired-end reads with an output of 6 G per sample. Gene ontology analysis was carried out using The Database for Annotation, Visualization and Integrated Discovery[107].

2.10. Statistical Analysis

Statistical analysis was done using GraphPad Prism 8 (GraphPad Software). The data is presented as mean ± standard error of the mean. The normality of the data was tested through Shapiro-Wilk test. The unpaired two-tailed Student's t-test and the Mann Whiteny test were the parametric and non-parametric test used respectively to compare two groups (control versus experimental). The time-course experiments only measured the statistical difference between the control and clodronate from the 3dpi with the previous test.

The number of replicates is indicated in the respective figures. To ensure statistical significance, the p-value was set at 0.05.

Results and Discussion

3. Results and Discussion

Skeletal muscle aging is characterized by a loss of regenerative capacity due to changes in the tissue environment, a reduction of muscle stem cells (MuSCs), and the accumulation of intrinsic defects in the remaining MuSC population[11,47].

Using a mouse model of immune dysfunction, Sousa et al. characterized age-related alterations in myeloid populations and showed that immune changes that mimic aging affected MuSC function[43]. However, the mechanisms underlying the impact of this unbalanced immune environment in MuSCs remain unknown.

Additionally, preliminary results at three days post-injury (3dpi) in aged mice and models of immune aging showed not only a decline in MuSC's number but also a cell fate change of some MuSCs into a new subpopulation of MuSCs characterized by the simultaneous expression of α7Integrin and Sca1. Moreover, experiments in the lab with lineage tracing technique demonstrated that the α7Integrin^{pos}Sca-1^{pos} population derive from Pax7 MuSCs. Transcriptomic analysis of this new population revealed increased gene expression related to interferon (IFN) response and with alternative lineage commitment.

This project aims to investigate the immune system's role in MuSC aging during regeneration and study the potential impact of interferon on MuSC behavior in young and aged skeletal muscle regeneration.

3.1. Macrophage ablation leads to a decline in the MuSC population at 3dpi

Sousa et al. demonstrated that the immune system's impairment, including the decline in the myeloid cell population (CD11b positive population) and the reduction in the MuSC's pool, co-occur in aging and MANF-deficient mice conditions[43]. In this work we administrated clodronate liposomes in the experimental group and PBS liposomes in the control group. The fundamental concept is that cells die through apoptosis when phagocytose clodronate liposomes[98]. Clodronate-treated mice environment recapitulate the aging environment since it promotes the decline in the immune cell population, as observed in aging. This recapitulation was validated in the Sousa et al. paper[43]. To understand the consequences of a dysfunctional immune system on the MuSC population, we study MuSC in clodronate-treated mice.

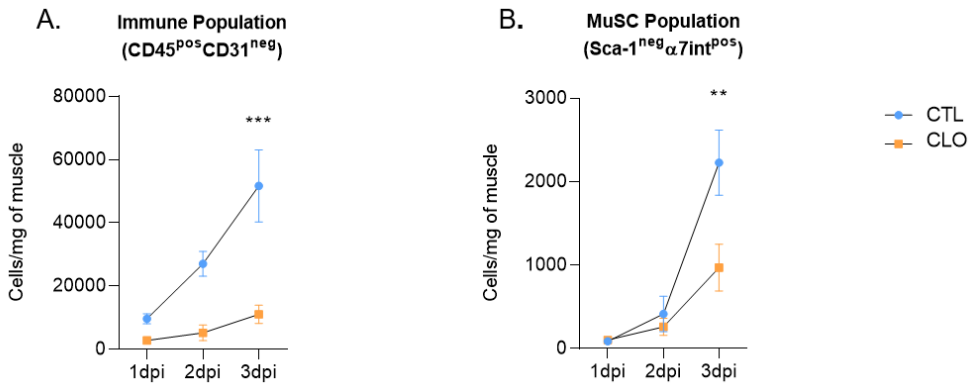

Figure 21. A. Quantification of the Immune Population in the first three days after injury in control and clodronate-treated groups. B. Quantification of the MuSC population in the first three days after injury both in control and clodronate-treated groups. Data was obtained by flow cytometry at different time points following injury in young mice. All data are presented as mean ± SEM. Normality was assessed for every group in each condition. The parametric unpaired t-test was performed in A and in B at 3dpi. For each time point considered it was used at least 3 samples collected from independent animals. **p<0.01 and ***p<0.001. dpi (days post-injury), CTL (control group), CLO (clodronate-treated group).

In **Figure 21A**, we compare the immune population ($CD45^{pos}CD31^{neg}$) at the first three days of skeletal muscle regeneration to evaluate the successful elimination of immune cells after clodronate treatment. Analysis showed that there was a significant decrease in the $CD45^{pos}$ population in the clodronate-treated group compared with the corresponding control at 3dpi. Considering that the macrophages are the prominent immune cell population in skeletal muscle regeneration[33] and the main phagocytic cell populations responsible for cleaning the tissue debris, including the dead cells (efferocytosis)[108], we can assume that the decrease of the immune population is associated to the decline of the macrophage population.

In this work, the immune population was reduced by (71,08%) on the first day post-injury, (80,96%) on the second day post-injury, and (78,68%) on the third day post-injury. Similar results were obtained in other published studies[109] where mice treated with clodronate liposomes experienced a decline of macrophages population ($F4/80^{pos}CD11b^{pos}$) by (73,2%), (80,2%), and (77,4%) on the three days following injury, respectively. These results support that the immune population's reduction is explained by the macrophage population's ablation and validate the use of clodronate-treated mice in this work.

The consequence of this prominent reduction of the macrophage population in MuSCs is displayed in **Figure 21B**. Analysis revealed that MuSC population was significantly declined in the clodronate-treated mice compared to the respective control group at 3dpi.

In addition to the debris clearance mentioned above, macrophages expand MuSC population and activate the myogenesis process, being critical intercellular communicators in the skeletal muscle regeneration process[33]. Since in the literature, clodronate-treated mice have smaller myofibers at 14dpi

conjugated with multiple necrotic fibers and inflammatory cells[109,110], we can suggest that MuSC population's natural response to injury at 3dpi depends on macrophages and in the absence of these cells, there is a defect in skeletal muscle regeneration through MuSC loss.

3.2. Macrophage ablation leads to an increase in MuSC death at 3dpi

To comprehend why the MuSC population disappeared from the skeletal muscle at 3dpi without macrophages, proliferation, cell death (apoptosis and loss of cell viability), and senescence activity in the MuSC population were assessed (**Figure 22**).

Proliferation was quantified by measuring the percentage of EdU (5-ethynyl-2'-deoxyuridine) positive cells. The EdU is a thymidine nucleoside analog that is incorporated into DNA during DNA synthesis[104]. Apoptosis was assessed by quantifying the Apopnexin Green dye that measures the phosphatidylserine (PS) relocation in the external membrane[100]. Cell death was assessed by measuring the amine-reactive signal[101] through the LIVE/DEAD signal. Amine reactive dye covalently binds to free cytoplasmatic amines in dead cells where the membrane was compromised[101]. Senescence was assessed by quantifying the SPiDER-βGal positive cells. The SPiDER-βGal probe binds to the β-galactosidase enzyme of the senescent cells, resulting in a fluorescent signal[102,103].

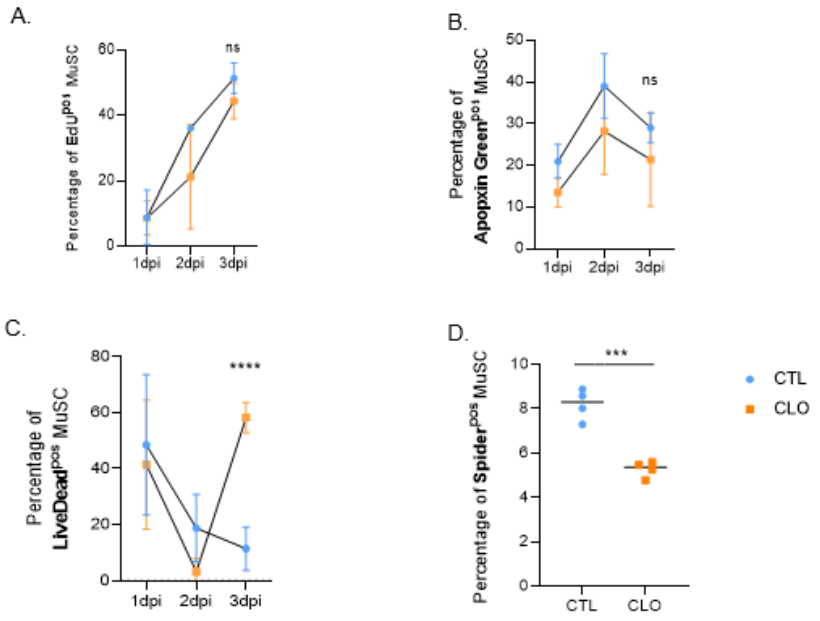

Figure 22. **MuSC profile during regeneration after macrophage ablation**. A. Percentage of EdU-positive MuSCs (proliferation marker). B. Percentage of Apopxin Green positive cells (apoptosis marker). C. Percentage of Live Dead positive cells (cell death marker). D. Percentage of SpiderB-Gal positive MuSC (senescence marker). Data obtained by flow cytometry following injury in young mice. Proliferation, Apoptosis, and Cell Death were assessed in the first three days of injury, while senescence was measured at 3dpi. The percentage of cells in each graph was calculated automatically by the FlowJo™ v10.8 Software (BD Life Sciences) software. All data are presented as mean ± SEM. Normality was assessed for every group in each condition. The parametric unpaired t-test was performed in graph A, B, C and D. At least three samples were collected from independent animals for each time

point considered. ***p<0.001 and ****p<0.0001. ns (non-significant), dpi (days post-injury), CTL (control group), CLO (clodronate group).

We did not observe any significant differences between the clodronate-treated group and the respective control group regarding proliferation and apoptosis at 3dpi (**Figures 22A and 22B**), suggesting that the proliferation and apoptosis do not explain the decline observed in the clodronate-treated group at 3dpi.

According to the literature, in homeostatic aged skeletal muscle, the MuSC become more senescent since there is a tendency to accumulate intracellular damage[111]. We tested whether eliminating the macrophages from the skeletal muscle after inducing injury could provoke an increase in senescent MuSCs. Unexpectedly, senescence activity was significantly less in the clodronate-treated group compared with the control at 3dpi (**Figure 22D**). This suggests that macrophages induced senescence in MuSC population during skeletal muscle regeneration at 3dpi. Therefore, this cell process is not the reason why MuSCs were significantly lost in the clodronate-treated group compared with the respective control group during skeletal muscle regeneration at 3dpi.

Further analysis showed a significantly increase in the percentage of dead MuSC in the clodronate-treated group compared to the respective control group at 3dpi (**Figure 22C**), suggesting that MuSCs disappear from the skeletal muscle in the clodronate-treated group due to an increase in cell death at 3dpi. Since there is no significant difference in the percentage of apoptotic cells between the control group and the clodronate-treated group at 3dpi (**Figure 22D**), cells are probably dying through a different type of cell death mechanism, such as necrosis.

To sum up, a significant increase in cell death can explain why MuSCs are lost from the skeletal muscle regeneration in the macrophage-ablated group compared with the control group at 3dpi. Further investigation on the specific type of cell death mechanism by which macrophages regulate the number of MuSCs at 3dpi requires assessment.

3.3. At 3dpi, some MuSCs from the clodronate-treated group became double positive for α7Integrin, and Sca-1, originating a new population in the skeletal muscle

MuSCs are characterized by being α7Integrin positive and Sca-1 negative[11,12]. Studies have shown that there is a small percentage of Sca-1 positive MuSC cells in the skeletal muscle in homeostatic conditions, contributing to the heterogeneity of the MuSC population[12,58].

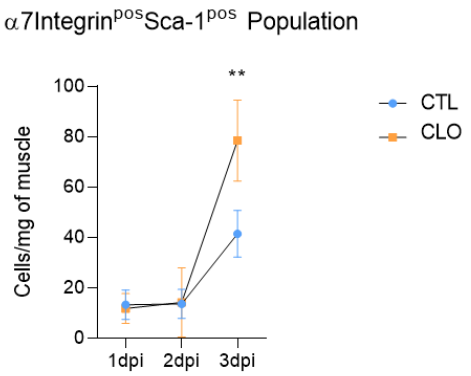

Figure 23. Number of α7integrin^{pos}SCA-1^{pos} cells in the QC muscle of young mice with macrophage ablation and corresponding control group, on a time course following skeletal muscle injury course. Data was obtained by flow cytometry at different time points following injury in young mice. All data are presented as mean ± SEM. Normality was assessed for every group, and the parametric unpaired t-test was performed. For each time point considered it was used at least 3 samples collected from independent animals. **p<0.01. dpi (days post-injury), CTL (control group), CLO (clodronate group).

Interestingly, we observed a significant increase in the MuSC subpopulation α7integrin^{pos}Sca-1^{pos} in the clodronate-treated group compared with the control at 3dpi, confirming previous findings from the lab showing that conditions of immune dysfunction promote the appearance of this rare MuSC subpopulation (**Figure 23**). Lineage tracing experiments results from the lab demonstrated that this new population (α7integrin^{pos}Sca-1^{pos}) was originated from the Pax7 MuSCs, suggesting a cell fate change in MuSC population at 3dpi. This cell fate change further explains the significant decline of MuSCs in the clodronate-treated group compared to the respective control group at 3dpi.

Concluding, these results suggest that MuSCs significantly disappear from the muscle in the clodronate-treated group compared to the control group due to the increase in cell death and a cell fate switch from α7Integrin^{pos}Sca-1^{neg} to α7Integrin^{pos}Sca-1^{pos} MuSC population at 3dpi.

Studies in the literature showed that without macrophages, the myogenesis-regulated cell process is compromised by declining the levels of MyoD and myogenin regulatory factors during skeletal muscle regeneration[109,112]. This impairment of the MuSC differentiation process with macrophage ablation could be partially explained by the increase in MuSC cell death and the change of the cell fate of MuSC at 3dpi, as we showed previously.

In preliminary results from the lab, the MuSC Sca-1 positive population also appeared in aged mice and MANF-deficient mice (preliminary results, results not showed), suggesting that a similar cell fate switch between those mice and the clodronate-treated mice. This supports the results obtained in this work suggesting that the microenvironment influences Sca-1 expression through a macrophage-regulated process.

3.4. α7Integrin^{pos}Sca-1^{pos} activity is not altered during the first three days of regeneration in the clodronate group

To understand the impact of macrophage ablation on the α7Integrin^{pos}Sca-1^{pos} population activity, the proliferation, apoptosis, cell death, and senescence were evaluated during the first three days of skeletal muscle regeneration, similarly to what was performed previously with the MuSC (α7Integrin^{pos}Sca-1^{neg}) population.

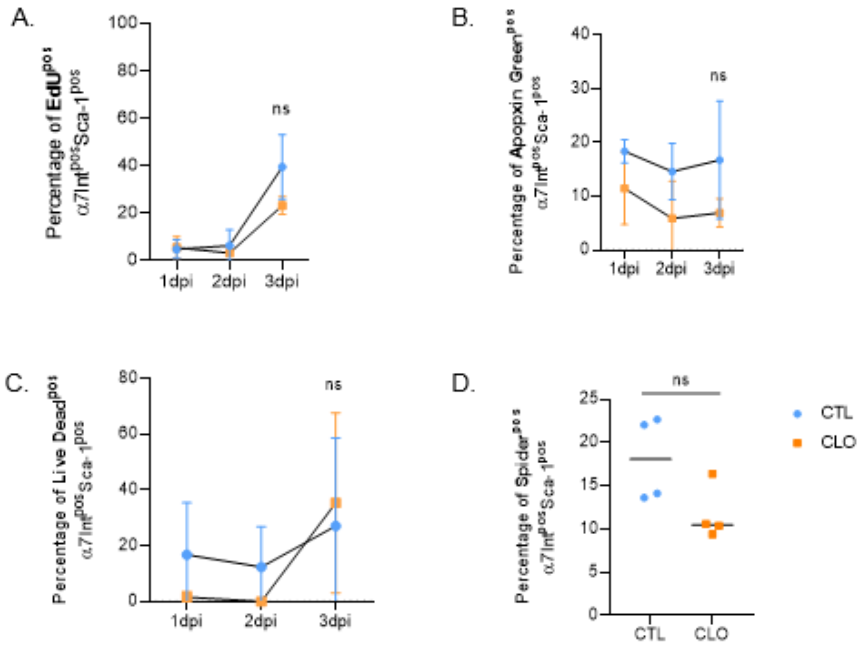

Figure 24. **Subpopulation of MuSC: α7integrin^{pos}SCA-1^{pos} activity profile after regeneration under control or in mice treated with clodronate liposomes**. A. Percentage of EdU positive MuSC (proliferation marker). B. Percentage of Apopxin Green positive cells (apoptosis marker). C. Percentage of Live Death positive cells (cell death marker). D. Percentage of Spiderβ-Gal positive MuSC (senescence marker). Data was obtained by flow cytometry following injury in young mice. Proliferation, Apoptosis, and Cell Death were assessed in the first three days of injury, while senescence was measured on the 3dpi. The percentage of cells in each graph was calculated automatically by the FlowJo™ v10.8 Software (BD Life Sciences) software. All data are presented as mean ± SEM. Normality was assessed for every group in each condition. The parametric unpaired t-test was performed in all graphs. At least three samples were collected from independent animals for each time point considered. ns (non-significant), dpi (days post-injury), CTL (control group), CLO (clodronate group).

There were no significant changes regarding the activity of proliferation, apoptosis, cell death and senescence in the α7Integrin^{pos}Sca-1^{pos} subpopulation of MuSC between the clodronate-treated group and the respective control group (**Figures 24A, 24B, 24C, and 24D**).

Concluding, in the absence of macrophages, there is a cell fate change of α7Integrin^{pos}Sca-1^{neg} population to α7Integrin^{pos}Sca-1^{pos} subpopulation. Furthermore, the α7Integrin^{pos}Sca-1^{pos} subpopulation

is not accumulating in the regenerating muscle due to an increase of its proliferative activity, or from a decrease in its apoptotic, senescence, and cell death rates.

3.5. Gene Ontology (GO) analysis revealed Interferon signaling as a potential driver of the α7integrin^{pos}SCA-1^{pos} state

To further understand the α7Integrin^{pos}Sca-1^{pos} population's trigger and function, we performed GO pathway analysis on the dataset of genes upregulated in the α7Integrin^{pos}Sca-1^{pos} vs α7Integrin^{pos}Sca-1^{neg} population, previously generated in the lab. In this experiment, a lineage-tracing methodology was used to ensure that the α7Integrin^{pos}Sca-1^{pos} population analyzed was originated from Pax7^{pos} cells in conditions of macrophage ablation to ensure they originate from “true” MuSCs .

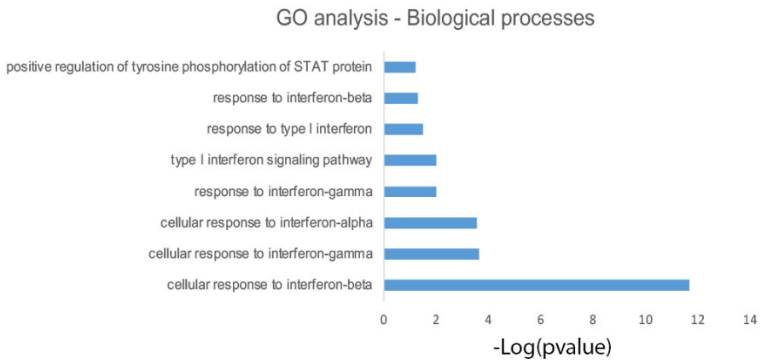

Figure 25. Gene ontology analysis. Gene ontology analysis of biological processes significantly enriched in the dataset of genes upregulated (fold change>5) in α7Integrin^{pos}Sca-1^{pos} vs α7Integrin^{pos}Sca-1^{neg} cells, isolated by FACS from mice at 3dpi. α7integrin^{pos}SCA-1^{pos} cells were isolated from clodronate-treated mice and α7Integrin^{pos}Sca-1^{neg} were isolated from control mice treated with PBS-liposomes. Cells were isolated from Pax7-TdTomato mice, which allows for lineage tracing of each population from “true” Pax7^{pos} MuSCs, identified by the expression of TdTomato protein.

Our analysis revealed an enrichment for interferon (IFN) signaling response in the dataset of genes upregulated in the α7integrin^{pos}SCA-1^{pos} population (**Figure 25**). Combining the gene ontology results with the fact that IFN induces Sca-1[113], the hypothesis formulated was that IFN could be a possible trigger for the appearance of α7integrin^{pos}SCA-1^{pos} population during regeneration without the macrophage population at 3dpi.

3.6. IFNα potentiates the switch between α7integrin^{pos}SCA-1^{neg} and α7integrin^{pos}SCA-1^{pos} population during regeneration

To test our hypothesis, IFNα was administered for two consecutive days after skeletal muscle injury, and the muscles were analyzed at 3dpi. α7Integrin^{pos}Sca1^{neg} and α7Integrin^{pos}Sca-1^{pos} populations were quantified (**Figures 26A and 26B**). Furthermore, to understand the impact of the interferon response on the immune system in the skeletal muscle at 3dpi, we analyzed the myeloid cells (**Figure 26C**), proinflammatory macrophages (**Figure 26D**), antiinflammatory/pro-repair macrophages (**Figure 26E**), and neutrophils populations (**Figure 26F**).

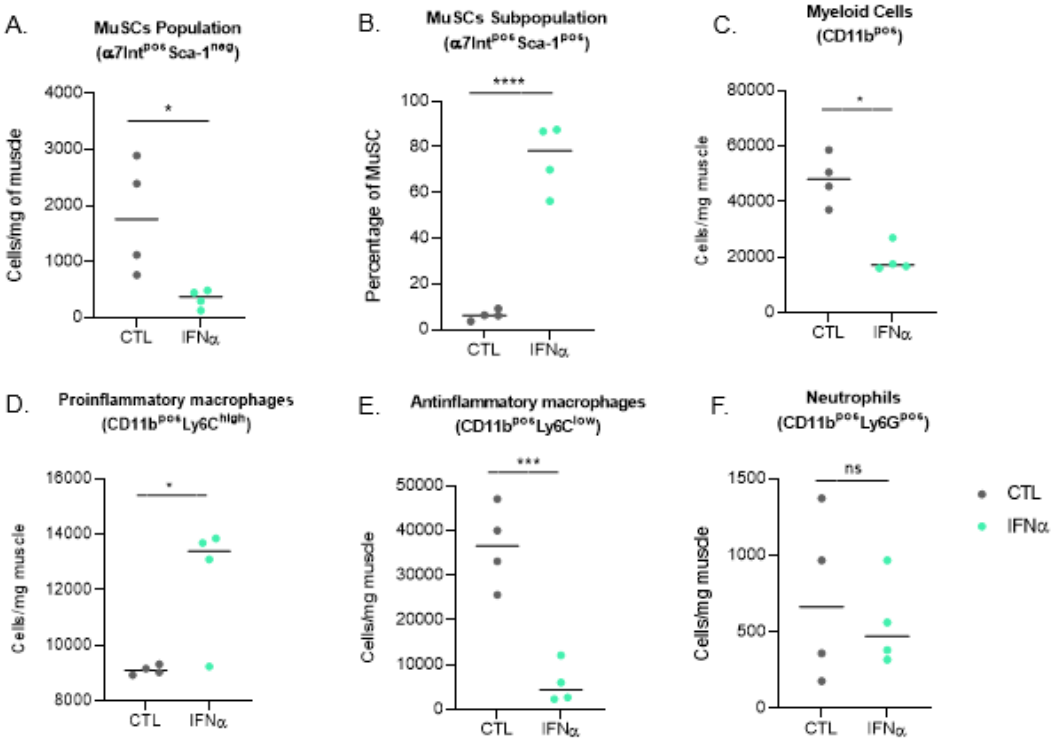

Figure 26. **The effect of IFNα in the α7Integrin^{pos}Sca-1^{neg}, α7Integrin^{pos}Sca-1^{pos}, and immune populations (Myeloid, Proinflammatory and anti-inflammatory macrophages, and neutrophils) in the control and clodronate treated groups at 3dpi**. A. Quantification of MuSC population. B. Percentage of the MuSC subpopulation α7Integrin^{pos}Sca-1^{pos}. The percentage was calculated manually by dividing the total number of α7Integrin^{pos}Sca-1^{pos} by the soma of α7Integrin^{pos}Sca-1^{neg} and α7Integrin^{pos}Sca-1^{pos} and multiplying per 100. Data was obtained by flow cytometry following injury in young mice. Administration of the Interferon was performed for two consecutive days after the injury. All data are presented as mean ± SEM. Normality was assessed for every group in each condition. The parametric unpaired t-test was performed in A, B, D, E and F. The non-parametric Mann Whiteny was used in graph C. For each time point considered, four samples were collected from independent animals. *p<0.05, **p<0.01, ***p<0.001, and ****p<0.0001. ns (non-significant), dpi (days post-injury), CTL (control group), IFNα (interferon alpha).

Analysis of the MuSC population revealed that there was a significant decline in α7Integrin^{pos}Sca-1^{neg} population and a significant increase in the proportion of α7Integrin^{pos}Sca-1^{pos} population in IFNα-treated mice compared to the respective control group at 3dpi (**Figures 26A and 26B**), suggesting a similar cell fate switch to what we observed in the mice treated with clodronate liposomes.

IFNα did not affect the cell death of α7Integrin^{pos}Sca-1^{neg} and α7Integrin^{pos}Sca-1^{pos} populations (**Annex 1**). Thus, this shows that the decline in MuSCs after treatment with IFNα is exclusively due to the transition from α7Integrin^{pos}Sca-1^{neg} to α7Integrin^{pos}Sca-1^{pos}. This suggests that IFNα treatment can be used as an experimental paradigm to study the MuSC cell fate switch without the confounding effect of cell death that is also present in the clodronate-treated mice.

Similar to what is described in the literature regarding myogenesis defects in macrophage ablation mice (mentioned above in result 3.3), researchers showed that IFNα impaired human and mouse myoblast cell lines differentiation *in vitro* by declining myogenin levels during regeneration[80]. However, since the MuSC cell death was not significantly altered in the IFNα-treated group compared with the control group at 3dpi, we can suggest that the MuSC's cell fate switch is one of the key mechanisms that impair MuSC's differentiation during skeletal muscle regeneration.

Furthermore, our results showed that IFNα dysregulated the immune system by reducing the myeloid population numbers (**Figure 26C**), recapitulating the immune dysfunctional system in aged mice and the clodronate-treated mice. While the anti-inflammatory population is also decreased in the IFNα-treated mice (**Figure 26E**), the proinflammatory macrophage population is significantly increased (**Figure 26D**), suggesting a macrophage phenotypic transition delay at 3dpi. There was no significant difference between the neutrophil population with the administration of the IFNα compared to the control group at 3dpi (**Figure 26F**).

To summarize this second part of the results, the IFNα stimulation delayed the phenotypic macrophage transition at 3dpi, recapitulating the phenotypic transition impairment in aged mice[43].

It is known that proinflammatory macrophages are more susceptible to IFNα signaling than antiinflammatory macrophages[114], suggesting that an overstimulation of proinflammatory macrophages by IFNα could be possibly accountable for the increment of this population. Interestingly, under an overstimulated IFNα environment, in the literature, HSC hematopoiesis activity increases[113,115], but there is a decline in the production of mature cells[113,115], possibly justifying the lack of myeloid cells upon IFNα administration at 3dpi.

3.7. IFNγ does not affect MuSCs during regeneration

Sca-1 is also strongly upregulated by interferon type II[116]. To clarify if the MuSC cell fate change was general or interferon type-specific, the effects of interferon-gamma (IFNγ) supplementation were also tested in the context of skeletal muscle regeneration at 3dpi.

The cell death analysis revealed that α7integrin^{pos}SCA-1^{neg} and α7integrin^{pos}SCA-1^{pos} populations had no significant differences comparing the IFNγ-treated mice and the respective control groups at 3dpi (**Anexo 2**). Furthermore, the cell fate of MuSCs was not significantly altered in the interferon-treated

mice compared to the respective control group at 3dpi (**Figures 27A and 27B**) since the changes in both α7integrin^{pos}SCA-1^{neg} and α7integrin^{pos}SCA-1^{pos} population were not significant between the two groups at 3dpi.

Analysis of the immune compartment revealed that the myeloid and the proinflammatory populations were significantly increased in IFNγ-treated mice compared to the respective control group at 3dpi (**Figure 27C and 27D**). However, the antiinflammaroy macrophage population and the neutrophils were not significantly altered comparing IFNγ-treated mice and the respective control mice at 3dpi (**Figure 27E and 27F**).

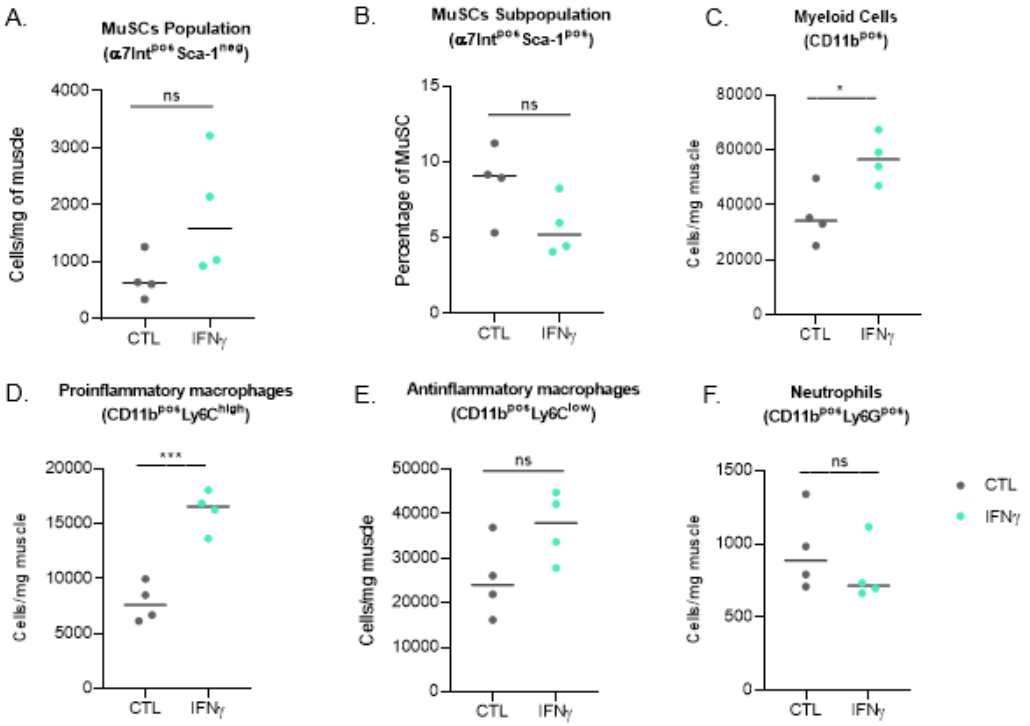

Figure 27. The effect of IFNγ in the α7Integrin^{pos}Sca-1^{neg}, α7Integrin^{pos}Sca-1^{pos}, and immune populations (Myeloid, Proinflammatory and anti-inflammatory macrophages, and neutrophils) in the control and clodronate treated groups at 3dpi. A. Quantification of MuSC population. B. Percentage of the MuSC subpopuplation α7Integrin^{pos}Sca-1^{pos}. The percentage was calculated manually by dividing the total number of α7integrin^{pos}SCA-1^{pos} by the soma of α7integrin^{pos}SCA-1^{neg} and α7integrin^{pos}SCA-1^{pos} and multiplying per 100. Data was obtained by flow cytometry following injury in young mice. Administration of the Interferon was performed for two consecutive days after the injury. All data are presented as mean ± SEM. Normality was assessed for every group in each condition. The parametric unpaired t-test was performed in A, B, C, D and E. The non-parametric Mann Whiteny was used in graph F. For each time point considered it was used 4 samples collected from independent animals. *p<0.05 and ***p<0.001. ns (non-significant), dpi (days post-injury), CTL (control group), IFNγ (interferon gamma).

The different behavior of the immune populations with the administration of the IFNα and IFNγ leads us to suggest that the mechanism of action regarding the immune system diverge. IFNγ does not

recapitulate the cell fate switch observed in clodronate-treated mice and IFNα treated mice. However, IFNγ provokes a proinflammatory immune system environment comparing with the control group during skeletal muscle regeneration at 3dpi.

Concluding, IFNα but not IFNγ induced the cell fate switch of the MuSC population from α7Integrin^{pos}Sca-1^{neg} to α7Integrin^{pos}Sca-1^{pos} at 3dpi.

3.8. Poly IC recapitulates the IFNα response at 3dpi

As mentioned before, proinflammatory macrophages' primary function is to clear debris by phagocytosis in the context of tissue regeneration[36]. This is essential for the macrophage transition of a proinflammatory to a pro-repair phenotype[36]. Cell debris is the biological waste that remains when a cell dies, an unavoidable byproduct of the cell life cycle[117], and external damage like a skeletal muscle injury potentiates it. During an injury, cellular lysis releases free short sequences of RNA and DNA[118].

We hypothesized that interferon response could be activated by the presence and accumulation of tissue debris in a scenario without the presence of macrophages (clodronate-treated mice). To test this hypothesis, we administrated in young mice the Polyriboinosinic-polyribocytidylic acid, also known as Poly IC, an artificial molecular structure that mimics viral double-stranded RNA sequences[119], and recapitulates cell debris.

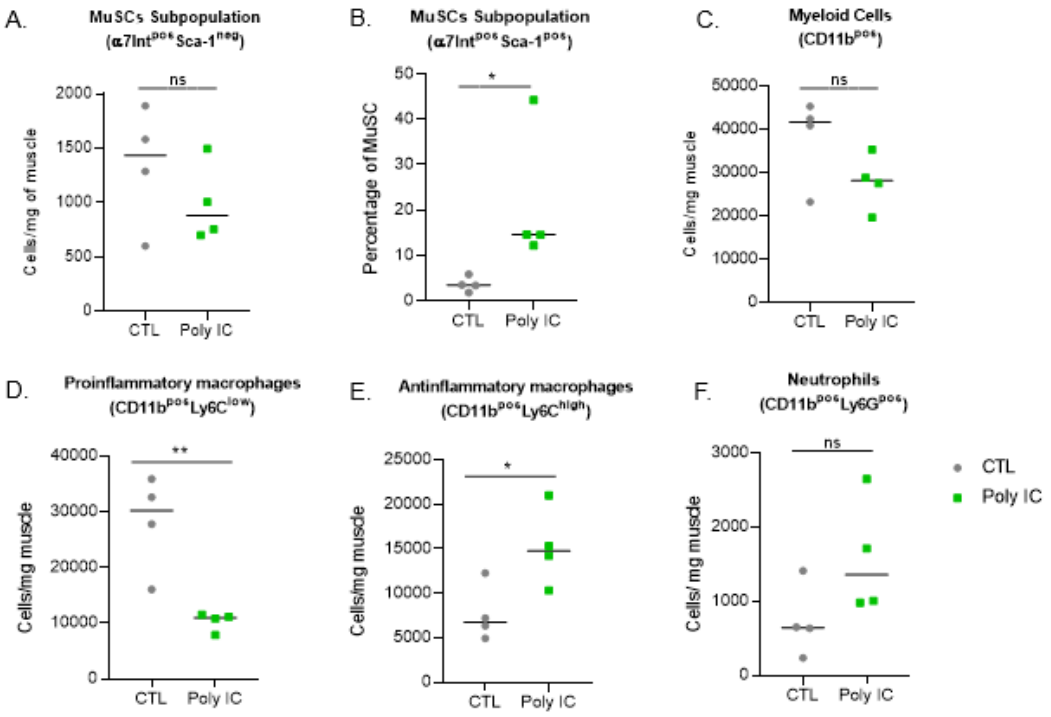

Figure 28. The effect of Poly IC in the α7Integrin^{pos}Sca-1^{neg}, α7Integrin^{pos}Sca-1^{pos}, and immune populations (Myeloid, Proinflammatory and anti-inflammatory macrophages, and neutrophils) in the control and clodronate treated groups at 3dpi. A. Quantification of MuSC population. B. Percentage of the MuSC

subpopulation α7integrin^{pos}SCA-1^{pos}. The percentage was calculated manually by dividing the total number of α7integrin^{pos}SCA-1^{pos} by the soma of α7integrin^{pos}SCA-1^{neg} and α7integrin^{pos}SCA-1^{pos} and multiplying per 100. C. Quantification of myeloid cells. D. Quantification of proinflammatory cells. D. E. Quantification of antiinflammatory cells. F. Quantification of neutrophils. Data was obtained by flow cytometry following injury in young mice. Administration of the Interferon was performed for two consecutive days after the injury. All data are presented as mean ± SEM. Normality was assessed for every group in each condition. The parametric unpaired t-test was performed in A, C, D, E and F. The non-parametric Mann Whiteny was used in graph B. For each time point considered, four samples were collected from independent animals. *p<0.05, **p<0.01 and ***p<0.001. dpi (days post-injury), ns (non-significant), CTL (control group), Polyinosinic–polycytidylic acid sodium salt (Poly IC).

Although the α7Integrin^{pos}Sca-1^{neg} MuSC population decline was not significant with Poly IC treatment compared with the control group at 3dpi (**Figure 28A**), there was a tendency for a decrease in the number of α7Integrin^{pos}Sca-1^{neg} population in the Poly IC-treated mice (1340,25 cells average/mg of muscle) compared with the controls to (989,1 cells average/mg of muscle). However, an increase in the number of mice used in each group is required to conclude this with confidence. On the other hand, our results showed a significant increase in the α7Integrin^{pos}Sca-1^{pos} population in the Poly IC-treated mice compared to the control group at 3dpi (**Figure 28B**), suggesting an almost identical cell fate switch to what we observed in the IFNα-treated mice and clodronate-treated mice.

According to the literature, Poly IC mediates cell-mediated immunity and a robust type I interferon response[120], further supporting that they share identical cell process mechanisms.

Analysis on the immune population revealed that the proinflammatory population was significant increased and the anti-inflammatory population was significantly reduced in the Poly IC-treated group compared with the respective control group at 3dpi (**Figure 28D and 28E**). Moreover, the myeloid cells and neutrophils were not significantly affected by the Poly IC treatment compared with the respective control group at 3dpi (**Figure 28C and 28F**).

To sum up, the phenotypic switch of MuSC from α7Integrin^{pos}Sca-1^{neg} to α7Integrin^{pos}Sca-1^{pos} and the delay of the macrophage phenotypic transition is promoted in the Poly IC treated group compared with the control group at 3dpi, mimicking the IFNα response.

3.9. IFNα acts directly in MuSC cells

To understand if the IFNα and Poly IC act directly on MuSC to provoke this phenotypic change or if they are inducing the α7Integrin^{pos}Sca-1^{pos} population through the altered immune system, *in vitro* experiments were performed.

C2C12 is a myoblast cell line that is a subclone (produced by H. Blau, et al) of the mouse myoblast cell line established by D. Yaffe and O. Saxel[121]. Mouse C2C12 muscle cells are the most used cellular model to mimic skeletal muscle *in vitro*[122].

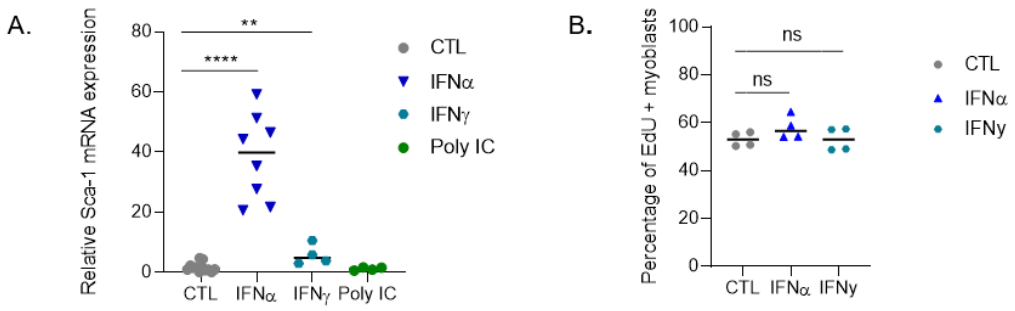

Figure 29. IFNα acts directly on C2C12 myoblasts in vitro. A. Relative Sca-1 mRNA expression in control myoblasts and after stimulation with IFNα, IFNy, and Poly IC. B. Analysis of the percentage of EdU-positive myeloblasts in the control group, IFNα-stimulated group and the IFNy-stimulated group. The percentage of cells in each graph was calculated automatically by the FlowJo™ v10.8 Software (BD Life Sciences) software. Data was obtained 24h after stimulation by RT-PCR in C2C12 myoblast cell culture lineage. **p<0.01, ****p<0.0001. ns (non-significant), CTL (control group), IFNα (interferon alpha), IFNγ (interferon gamma), Polyinosinic–polycytidylic acid sodium salt (Poly IC).

IFNα, IFNγ and Poly IC were administrated directly into the C2C12, and RTq-PCR measured Sca-1 expression levels. Despite IFNα potentiating a modified immune system, it significantly increased the Sca-1 expression levels in C2C12 compared with the control group at 24h of stimulation, suggesting that the IFNα acts directly on MuSC to change the cell fate (**Figure 29A**).

Surprisingly, IFNγ significantly increased the Sca-1 levels in C2C12 compared with the control group at 24h of stimulation, contrary to the *in vivo* results. Since we obtained an *in vitro* positive result and IFNγ is reported to impair myogenesis[123], this could mean that possibly the *in vivo* concentration used was insufficient for causing myogenesis impairment through the MuSC cell fate switch. Further experiments with higher doses *in vivo* should be tested to clarify the effect of the IFNγ in the MuSC population *in vivo*.

Poly IC did not affect the expression levels of Sca-1 in C2C12 compared with the control at 24h of stimulation (**Figure 29A**). This implies that Poly IC is not acting directly on MuSC to promote the cell fate switch in an autocrine way. Instead, Poly IC induces other cell types to produce interferon that activates the MuSC to change cell fate.

These changes in the Sca-1 expression happened without changing the C2C12 proliferation activity in the interferon-treated groups compared with the respective control group at 24h of stimulation (**Figure 29B**).

Poly IC is a TLR3 agonist[124,125]. The receptor TLR3 is expressed in the membrane of B-cells, macrophages, and dendritic cells having a prominent effects in CD8+ T cells and natural killers[124,125]. Since plasmacytoid dendritic cells are known to produce IFNα[77] and T cells (CD4+ and CD8+) are known

to produce IFNγ[77,80], possibly Poly IC could be acting directly on plasmacytoid dendritic cells and T cells to promote the increase in interferon and trigger the interferon-related response.

However, further experiments need to be performed to unravel the identities of the cells responsible for interferon production upon stimulation with Poly IC or cellular debris, in the context of skeletal muscle regeneration.

3.10. JAK-STAT pathway mediates the effects of INFα *in vitro*

Despite IFNα directly provoking the increase in Sca-1 in MuSC compared with the control group at 24h of stimulation, the signaling pathway remains unknown. Gene ontology analysis highlights the JAK-STAT pathway as an overstimulated pathway in the Sca-1 positive MuSC population. Since the JAK-STAT signaling cues are the main interferon-activated response[83,126,127], we hypothesized that this could be the activated pathway that induced Sca-1 stimulation. We focus exclusively on IFNα since it was the only interferon that provoked the cell fate change both *in vitro* and *in vivo*.

To test this, we used the Ruxolitinib JAK-STAT inhibitor. Ruxolitinib belongs to the first generational Jakinibs family and strongly inhibits the JAK1 and JAK2 inhibitors[83]. It has a moderate function, blocking the TYK2 receptor[83].

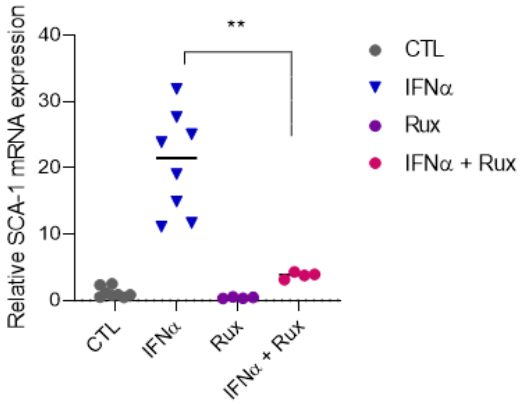

Figure 30. JAK-STAT pathway stimulates Sca-1 induction. Relative Sca-1 mRNA expression regarding CTL, IFNα, Rux, and IFNα + Rux. Data was obtained 24h after stimulation by RT-PCR in C2C12 myoblast cell culture lineage. **p<0.01. ns (non-significant), CTL (control group), IFNα (interferon alpha), Rux (Ruxolitinib), (IFNα + Rux) Interferon alpha and Ruxolitinib.

Analysis of the Sca-1 mRNA expression revealed that there was a significant decline in the IFNα+Rux compared with the IFNα group at 24h of stimulation, suggesting that Sca-1 is induced by an IFNα JAK-STAT pathway response (**Figure 30**). A representative model of the MuSC cell fate change process is schematized in the **Figure 31**.

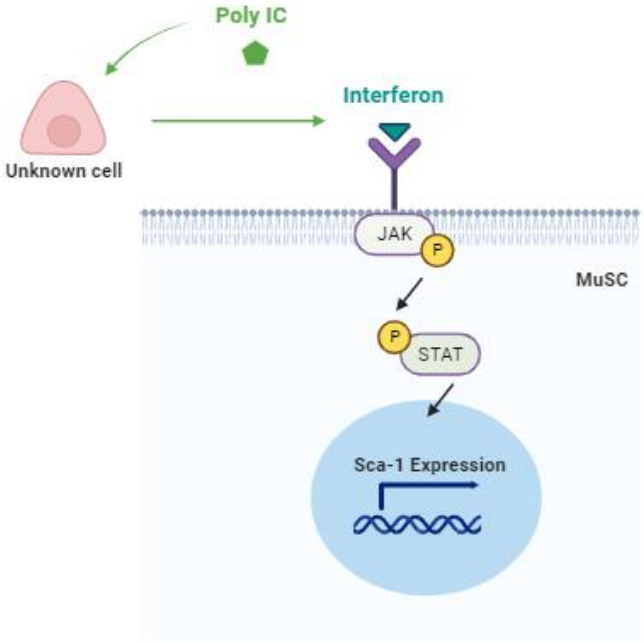

Figure 31. **Representative scheme regarding the MuSC cell fate switch from α7Integrin^{pos}Sca-1^{neg} to α7Integrin^{pos}Sca-1^{pos} population**. Poly IC induces the interferon production in an unknown cell that will activate the MuSC. Through the JAK-STAT pathway activation, Sca-1 expression levels increase, producing a behavior change in MuSC.

3.11. IFNα modifies the skeletal muscle regenerative success at 14dpi

To understand the long-term consequences of IFNα in skeletal muscle regeneration, IFNα was administrated as previously done, and mice were sacrificed at 14dpi.

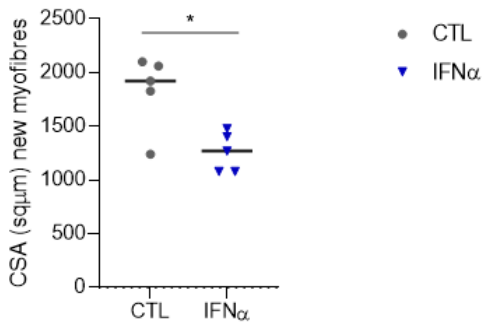

Figure 32. **Quantification of average CSA (sqμm) of new myofibers from TA muscles in the control and the IFNα at 14 dpi**. Data was obtained by quantifying the CSA of each muscle in the ImageJ software. Administration of the IFNα was performed for two consecutive days after the injury. All data are presented as mean ± SEM. For each time point considered, five samples were collected from independent animals. *p<0.05. CTL (control group), IFNα (interferon alpha), CSA (cross-section area).

Results showed that there is a significant decline in the cross-section area of the myofibers with IFNα treatment compared to the control group at 14dpi (**Figure 32**), suggesting that IFNα impairs the skeletal muscle regeneration.

As mentioned in the literature, IFNα impairs human and mouse myoblast cell lines differentiation *in vitro* by declining the myogenin levels during regeneration[80]. Since the effect of administrating IFNα *in vivo* during skeletal muscle regeneration significantly impaired myofiber formation during regeneration (**Figure 32**), we can hypothesize a mode of action involving the impairment in the myogenesis process. Although the role of the Sca-1 positive population is unclear in the literature, a study revealed that this population had a slower dividing profile and did not form myotubes as instantly as the negative population[58], being characterized by presenting an almost MuSC "quiescent" phenotype-like. Probably, the cell fate switch from α7Integrin^{pos}Sca-1^{neg} to α7Integrin^{pos}Sca-1^{pos} populations promoted by IFNα impaired the myogenesis process by declining the myogenic ability of MuSCs.

Conclusion and Future Perspectives

4. Conclusion and Future Perspectives

This project studied the **consequences of a dysfunctional immune system in MuSC during skeletal muscle regeneration**. Treatment with clodronate liposomes was used to mimic the aging dysfunctional immune system. We demonstrated that, in conditions of immune dysfunction, MuSCs (α7Integrin^{pos}Sca-1^{neg}) disappeared from the muscle at 3dpi due to an **increase in cell death** and a **cell fate change** from α7Integrin^{pos}Sca-1^{neg} to α7Integrin^{pos}Sca-1^{pos} MuSC population. This cell fate transition was demonstrated to happen in aging as well (preliminary data, data not shown).

Through gene ontology analysis, **Interferon** was suggested to be a possible candidate to promote this cell fate switch in MuSC at 3dpi.

Our results support a mechanism by which interferon induces **Sca-1 gene expression** production. Firstly, due to the lack of macrophages in the skeletal muscle site of regeneration, there is an **accumulation of debris** (which can be mimicked by Poly I:C treatment), which is going to stimulate interferon production in an unknown cell. This interferon signal activates the MuSC through the **JAK-STAT pathway** to induce Sca-1 levels. This mechanism is a plausible explanation for the MuSC cell fate switch in the clodronate-treated mice and IFNα-treated mice.

It is known that in aged skeletal muscle, MuSCs function and the immune system are impaired[11]. However, there is no evidence that IFNα levels increase with aging in the skeletal muscle, and there is even a decline in macrophage-specific IFN-γ response[70]. Further studies should be conducted to test whether IFNα and IFNγ concentration increase in skeletal muscle aging after an injury.

One interesting future perspective is to test IL-6 as a possible candidate for promoting the MuSC cell fate change in the aged skeletal muscle.

Firstly, IL-6 is a proinflammatory cytokine increased in aging that can activate the JAK1-STAT1-STAT3[83] and secondly, IL-6 expression is induced in myoblasts by Poly IC treatment[128]. The activation of STAT1 by Il-6 is less pronounced than other molecules mainly because IL-6 provokes a transient activation of STAT1 kinetics[91]. However, since the significant increase of the α7Integrint^{pos}Sca-1^{pos} population that occurred in the clodronate group and in aged mice compared to the control was by approximately 5% comparatively to the cell fate switch that happened in the IFNα-treated mice under the same conditions (80%), we can hypothesized that IL-6 could be a candidate for the small cell fate switch in the clodronate-treated group and in aging.

Lineage tracing experiments could be interesting to perform in an IFNα stimulated muscle at 7dpi and 14dpi, to evaluate the cell fate switch long-term outcome. Moreover, to study the effect of Sca-1 positive MuSC transplant experiments could be performed in homeostasis, clodronate treated and aged stem cell niche. Furthermore, since the intracellular pathways involved in the cell fate switch originating Sca-1 positive MuSCs in the muscle *in vivo* are still unknown general and specific JAK-STAT inhibitors should be tested.

The relevance of this work relies on discovering the cell fate switch mechanism behind the loss of MuSCs in aging through a macrophage-mediated process. This opens doors to further experiments and follow-up projects to unravel the clinical relevance of this finding in aging and possibly contribute to developing new, more accurate, and effective regenerative therapies.

Annex

5. Annex

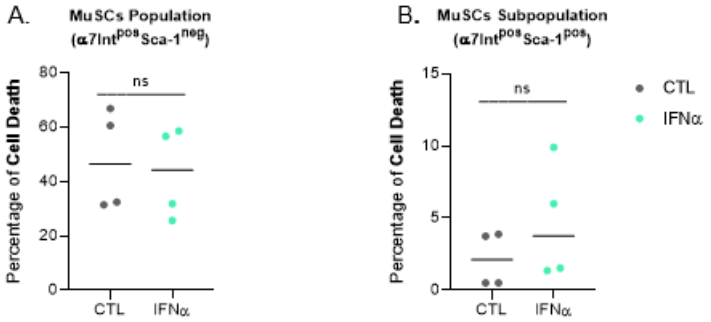

Annex 1. IFNα did not affect the cell death of α7integrin^{pos}SCA-1^{neg} and α7integrin^{pos}SCA-1^{pos} populations. A. Percentage of MuSC α7Integrin^{pos}Sca-1^{neg} population. B. Percentage of the MuSC α7Integrin^{pos}Sca-1^{pos} population. Data was obtained by flow cytometry following injury in young mice. Administration of the IFNα was performed for two consecutive days after the injury. All data are presented as mean ± SEM. For each time point considered, four samples were collected from independent animals. ns (non-significant), CTL (control group), IFNα (Interferon alpha).

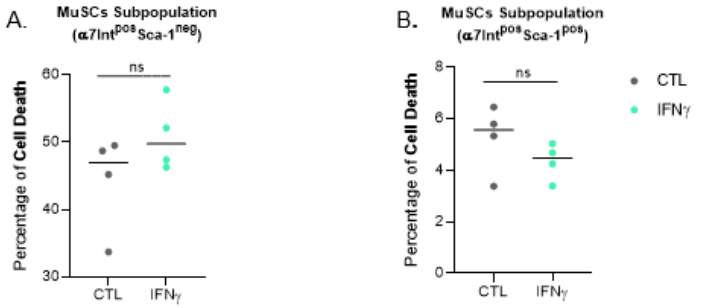

Annex 2. IFNγ did not affect the cell death of α7Integrin^{pos}Sca-1^{neg} and α7Integrin^{pos}Sca-1^{pos} populations. A. Percentage of MuSC α7Integrin^{pos}Sca-1^{neg} population. B. Percentage of the MuSC α7Integrin^{pos}Sca-1^{pos} population. Data obtained by flow cytometry following injury in young mice. Administration of the IFNγ was performed for two consecutive days after the injury. All data are presented as mean ± SEM. For each time point considered, four samples were collected from independent animals. ns (non-significant), CTL (control group), IFNγ (Interferon gamma).

References

6. References

1. Wilmoth, J. R. *et al. World social report 2023 : leaving no one behind in an ageing world*. (2023).
2. Guo, J. *et al.* Aging and aging-related diseases: from molecular mechanisms to interventions and treatments. *Signal Transduct. Target. Ther.* **7**, (2022).
3. Janac, S., Clarke, B. & Gems, D. Aging: Natural or Disease? A View from Medical Textbooks. *RSC Drug Discov. Ser.* **2017**-**Janua**, 1–19 (2017).
4. López-Otín, C., Blasco, M. A., Partridge, L., Serrano, M. & Kroemer, G. The Hallmarks of Aging Europe PMC Funders Group. *Cell* **153**, 1194–1217 (2013).
5. Schmauck-Medina, T. *et al.* New hallmarks of ageing: a 2022 Copenhagen ageing meeting summary. *Aging (Albany. NY).* **14**, 6829–6839 (2022).
6. Leonardi, G. C., Accardi, G., Monastero, R., Nicoletti, F. & Libra, M. Ageing: From inflammation to cancer. *Immun. Ageing* **15**, 1–7 (2018).
7. Shapiro, H., Thaiss, C. A., Levy, M. & Elinav, E. The cross talk between microbiota and the immune system: Metabolites take center stage. *Curr. Opin. Immunol.* **30**, 54–62 (2014).
8. Neves, J. & Sousa-Victor, P. Regulation of inflammation as an anti-aging intervention. *FEBS J.* **287**, 43–52 (2020).
9. Duong, L. *et al.* Macrophage function in the elderly and impact on injury repair and cancer. *Immun. Ageing* **18**, 1–11 (2021).
10. Neves, J., Sousa-Victor, P. & Jasper, H. Rejuvenating Strategies for Stem Cell-Based Therapies in Aging. *Cell Stem Cell* **20**, 161–175 (2017).
11. Sousa-Victor, P., García-Prat, L. & Muñoz-Cánoves, P. Control of satellite cell function in muscle regeneration and its disruption in ageing. *Nat. Rev. Mol. Cell Biol.* **23**, 204–226 (2022).
12. Yin, H., Price, F. & Rudnicki, M. A. Satellite cells and the muscle stem cell niche. *Physiol. Rev.* **93**, 23–67 (2013).
13. Loghlen, A. O. The potential of aging rejuvenation ABSTRACT. *Cell Cycle* **21**, 111–116 (2022).
14. PUNT, A. & SCHIPPERS, B. The influence of light on the acetylcholine-contracture. *Acta Physiol. Pharmacol. Neerl.* **5**, 215–216 (1956).
15. Harrison e., D. & Archer, J. R. Genetic differences in effects of food restriction on aging in mice. *J. Nutr.* **117**, 376–382 (1987).
16. Klass, M. R. A method for the isolation of longevity mutants in the nematode Caenorhabditis elegans and initial results. *Mech. Ageing Dev.* **22**, 279–286 (1983).

17. Joanisse, S., Nederveen, J. P., Snijders, T., McKay, B. R. & Parise, G. Skeletal Muscle Regeneration, Repair and Remodelling in Aging: The Importance of Muscle Stem Cells and Vascularization. *Gerontology* **63**, 91–100 (2016).

18. Gayraud-Morel, B., Chrétien, F. & Tajbakhsh, S. Skeletal muscle as a paradigm for regenerative biology and medicine. *Regen. Med.* **4**, 293–319 (2009).

19. Christopher McCuller 1, Rishita Jessu 2, A. L. C. 3. *Physiology, Skeletal Muscle*. (StatPearls Publishing, Treasure Island (FL), 2023).

20. Frontera, W. R. & Ochala, J. Skeletal Muscle: A Brief Review of Structure and Function. *Behav. Genet.* **45**, 183–195 (2015).

21. Pedersen, B. K. & Febbraio, M. A. Muscles, exercise and obesity: Skeletal muscle as a secretory organ. *Nat. Rev. Endocrinol.* **8**, 457–465 (2012).

22. Isaac, A. R., Lima-filho, R. A. S. & Lourenco, M. V. Neuropharmacology How does the skeletal muscle communicate with the brain in health and disease ? *Neuropharmacology* **197**, 108744 (2021).

23. Wang, Z. *et al.* Article The molecular basis for sarcomere organization in vertebrate skeletal muscle ll ll The molecular basis for sarcomere organization in vertebrate skeletal muscle. *Cell* **184**, 2135-2150.e13 (2021).

24. Sciorati, C., Rigamonti, E., Manfredi, A. A. & Rovere-Querini, P. Cell death, clearance and immunity in the skeletal muscle. *Cell Death Differ.* **23**, 927–937 (2016).

25. Williams, G. N., Higgins, M. J. & Michael, D. Aging Skeletal Muscle : Physiologic. *Phys Ther* **82**, 62–68 (2002).

26. Tieland, M., Trouwborst, I. & Clark, B. C. Skeletal muscle performance and ageing. *J. Cachexia. Sarcopenia Muscle* **9**, 3–19 (2018).

27. Larsson, L. *et al.* Sarcopenia: Aging-related loss of muscle mass and function. *Physiol. Rev.* **99**, 427–511 (2019).

28. Lexell, J., Taylor, C. C. & Sjöström, M. What is the cause of the ageing atrophy?. Total number, size and proportion of different fiber types studied in whole vastus lateralis muscle from 15- to 83-year-old men. *J. Neurol. Sci.* **84**, 275–294 (1988).

29. Akima, H. *et al.* Muscle function in 164 men and women aged 20-84 yr. *Med. Sci. Sports Exerc.* **33**, 220–226 (2001).

30. McCormick, R. & Vasilaki, A. Age-related changes in skeletal muscle: changes to life-style as a therapy. *Biogerontology* **19**, 519–536 (2018).

31. Morton, A. B. *et al.* Barium chloride injures myofibers through calcium-induced proteolysis with fragmentation of motor nerves and microvessels. *Skelet. Muscle* **9**, 1–10 (2019).

32. Hardy, D. *et al.* Comparative study of injury models for studying muscle regeneration in mice. *PLoS One* **11**, 1–24 (2016).

33. Chazaud, B. Inflammation and Skeletal Muscle Regeneration: Leave It to the Macrophages! *Trends Immunol.* **41**, 481–492 (2020).

34. Waldemer-Streyer, R. J., Kim, D. & Chen, J. Muscle cell-derived cytokines in skeletal muscle regeneration. *FEBS J.* **289**, 6463–6483 (2022).

35. Oishi, Y. & Manabe, I. Macrophages in inflammation, repair and regeneration. *Int. Immunol.* **30**, 511–528 (2018).

36. Arnold, L. *et al.* Inflammatory monocytes recruited after skeletal muscle injury switch into antiinflammatory macrophages to support myogenesis. *J. Exp. Med.* **204**, 1057–1069 (2007).

37. Peiseler, M. & Kubes, P. More friend than foe: The emerging role of neutrophils in tissue repair. *J. Clin. Invest.* **129**, 2629–2639 (2019).

38. Sousa-victor, P. & Neves, J. Immune dysregulation and skeletal muscle regenerative failure in aging. 1–30.

39. Ochoa, O. *et al.* Delayed angiogenesis and VEGF production in CCR2-/- mice during impaired skeletal muscle regeneration. *Am. J. Physiol. - Regul. Integr. Comp. Physiol.* **293**, 651–661 (2007).

40. Martinez, C. O. *et al.* Regulation of skeletal muscle regeneration by CCR2-activating chemokines is directly related to macrophage recruitment. *Am. J. Physiol. - Regul. Integr. Comp. Physiol.* **299**, 832–842 (2010).

41. Latroche, C. *et al.* Coupling between Myogenesis and Angiogenesis during Skeletal Muscle Regeneration Is Stimulated by Restorative Macrophages. *Stem Cell Reports* **9**, 2018–2033 (2017).

42. Juban, G. *et al.* AMPK Activation Regulates LTBP4-Dependent TGF-β1 Secretion by Pro-inflammatory Macrophages and Controls Fibrosis in Duchenne Muscular Dystrophy. *Cell Rep.* **25**, 2163-2176.e6 (2018).

43. Neves, J. & Sousa-victor, P. Aging disrupts MANF-mediated immune modulation during skeletal muscle regeneration. (2023) doi:10.1038/s43587-023-00382-5.

44. Tidball, J. G. Regulation of muscle growth and regeneration by the immune system. *Nat. Rev. Immunol.* **17**, 165–178 (2017).

45. MAURO, A. Satellite cell of skeletal muscle fibers. *J. Biophys. Biochem. Cytol.* **9**, 493–495 (1961).

46. Wang, Y. X., Dumont, N. A. & Rudnicki, M. A. Muscle stem cells at a glance. *J. Cell Sci.* **127**, 4543–4548 (2014).

47. Yamakawa, H., Kusumoto, D., Hashimoto, H. & Yuasa, S. Stem cell aging in skeletal muscle regeneration and disease. *Int. J. Mol. Sci.* **21**, (2020).

48. Relaix, F. *et al.* Pax3 and Pax7 have distinct and overlapping functions in adult muscle progenitor cells. *J. Cell Biol.* **172**, 91–102 (2006).

49. Yu, D. *et al.* Myogenic Differentiation of Stem Cells for Skeletal Muscle Regeneration. *Stem Cells Int.* **2021**, (2021).

50. Hernández-Hernández, J. M., García-González, E. G., Brun, C. E. & Rudnicki, M. A. The myogenic regulatory factors, determinants of muscle development, cell identity and regeneration. *Semin. Cell Dev. Biol.* **72**, 10–18 (2017).

51. Wang, R. *et al.* MyoD is a 3D genome structure organizer for muscle cell identity. *Nat. Commun.* **13**, 1–17 (2022).

52. Rayagiri, S. S. *et al.* Basal lamina remodeling at the skeletal muscle stem cell niche mediates stem cell self-renewal. *Nat. Commun.* **9**, 1–12 (2018).

53. Archacka, K. *et al.* Beneficial Effect of IL-4 and SDF-1 on Myogenic Potential of Mouse and Human Adipose Tissue-Derived Stromal Cells. *Cells* **9**, (2020).

54. Shivtiel, S. *et al.* CD45 regulates retention, motility, and numbers of hematopoietic progenitors, and affects osteoclast remodeling of metaphyseal trabecules. *J. Exp. Med.* **205**, 2381–2395 (2008).

55. Liu, L. & Shi, G. P. CD31: Beyond a marker for endothelial cells. *Cardiovasc. Res.* **94**, 3–5 (2012).

56. Te, L. J. I., Doherty, C., Correa, J. & Batt, J. Identification, isolation, and characterization of fibro-adipogenic progenitors (Faps) and myogenic progenitors (mps) in skeletal muscle in the rat. *J. Vis. Exp.* **2021**, 1–32 (2021).

57. Burkin, D. J. & Kaufman, S. J. The α7β1 integrin in muscle development and disease. *Cell Tissue Res.* **296**, 183–190 (1999).

58. Mitchell, P. O. *et al.* Sca-1 negatively regulates proliferation and differentiation of muscle cells. *Dev. Biol.* **283**, 240–252 (2005).

59. Giuliani, G. *et al.* SCA-1 micro-heterogeneity in the fate decision of dystrophic fibro/adipogenic progenitors. *Cell Death Dis.* **12**, 1–24 (2021).

60. Dumont, N. A., Wang, Y. X. & Rudnicki, M. A. Intrinsic and extrinsic mechanisms regulating satellite cell function. *Dev.* **142**, 1572–1581 (2015).

61. Henze, H., Jung, M. J., Ahrens, H. E., Steiner, S. & von Maltzahn, J. Skeletal muscle aging – Stem cells in the spotlight. *Mech. Ageing Dev.* **189**, 111283 (2020).

62. Fry, C. S. *et al.* Inducible depletion of satellite cells in adult, sedentary mice impairs muscle

regenerative capacity without affecting sarcopenia. *Nat. Med.* **21**, 76–80 (2015).

63. Olesen, A. T. *et al.* Age-related myofiber atrophy in old mice is reversed by ten weeks voluntary high-resistance wheel running. *Exp. Gerontol.* **143**, 111150 (2021).

64. Price, F. D. *et al.* Inhibition of JAK-STAT signaling stimulates adult satellite cell function. *Nat. Med.* **20**, 1174–1181 (2014).

65. Sousa-Victor, P., Perdiguero, E. & Muñoz-Ćanoves, P. Geroconversion of aged muscle stem cells under regenerative pressure. *Cell Cycle* **13**, 3183–3190 (2014).

66. Collins, C. A., Zammit, P. S., Ruiz, A. P., Morgan, J. E. & Partridge, T. A. A Population of Myogenic Stem Cells That Survives Skeletal Muscle Aging. *Stem Cells* **25**, 885–894 (2007).

67. Conboy, I. M. *et al.* Conboy, 2005, Nature, Rejuvenecimento celular e nicho.pdf. *Nature* **433**, 760–764 (2005).

68. Tidball, J. G., Flores, I., Welc, S. S., Wehling-Henricks, M. & Ochi, E. Aging of the immune system and impaired muscle regeneration: A failure of immunomodulation of adult myogenesis. *Exp. Gerontol.* **145**, 111200 (2021).

69. Wang, Y. *et al.* Aging of the immune system causes reductions in muscle stem cell populations, promotes their shift to a fibrogenic phenotype, and modulates sarcopenia. *FASEB J.* **33**, 1415–1427 (2019).

70. Zhang, C. *et al.* Age-related decline of interferon-gamma responses in macrophage impairs satellite cell proliferation and regeneration. *J. Cachexia. Sarcopenia Muscle* **11**, 1291–1305 (2020).

71. Ratnayake, D. *et al.* Macrophages provide a transient muscle stem cell niche via NAMPT secretion. *Nature* **591**, 281–287 (2021).

72. Kuswanto, W. *et al.* Poor Repair of Skeletal Muscle in Aging Mice Reflects a Defect in Local, Interleukin-33-Dependent Accumulation of Regulatory T Cells. *Immunity* **44**, 355–367 (2016).

73. Taylor-Jones, J. M. *et al.* Activation of an adipogenic program in adult myoblasts with age. *Mech. Ageing Dev.* **123**, 649–661 (2002).

74. Brack, A. S. *et al.* Increased Wnt signaling during aging alters muscle stem cell fate and increases fibrosis. *Science (80-.).* **317**, 807–810 (2007).

75. Isaacs, A. & Lindenmann, J. Virus interference. I. The interferon. *Proc. R. Soc. London. Ser. B - Biol. Sci.* **147**, 258–267 (1957).

76. Walter, M. R. The Role of Structure in the Biology of Interferon Signaling. *Front. Immunol.* **11**, 1–12 (2020).

77. Barrat, F. J. *et al.* Interferon target-gene expression and epigenomic signatures in health and

disease. **20**, 1574–1583 (2020).

78. Wack, A., Terczyńska-Dyla, E. & Hartmann, R. Guarding the frontiers: The biology of type III interferons. *Nat. Immunol.* **16**, 802–809 (2015).

79. Lee, A. J. & Ashkar, A. A. The dual nature of type I and type II interferons. *Front. Immunol.* **9**, 1–10 (2018).

80. Bolko, L. *et al.* The role of interferons type I, II and III in myositis: A review. *Brain Pathol.* **31**, 1–13 (2021).

81. Londhe, P. & Davie, J. K. Gamma Interferon Modulates Myogenesis through the Major Histocompatibility Complex Class II Transactivator, CIITA. *Mol. Cell. Biol.* **31**, 2854–2866 (2011).

82. Zhuang, S., Russell, A., Guo, Y., Xu, Y. & Xiao, W. IFN-γ blockade after genetic inhibition of PD-1 aggravates skeletal muscle damage and impairs skeletal muscle regeneration. *Cell. Mol. Biol. Lett.* **28**, (2023).

83. Hu, X., li, J., Fu, M., Zhao, X. & Wang, W. The JAK/STAT signaling pathway: from bench to clinic. *Signal Transduct. Target. Ther.* **6**, (2021).

84. Clark, J. D., Flanagan, M. E. & Telliez, J. B. Discovery and development of Janus kinase (JAK) inhibitors for inflammatory diseases. *J. Med. Chem.* **57**, 5023–5038 (2014).

85. Schoggins, J. W. Interferon-Stimulated Genes: What Do They All Do? *Annu. Rev. Virol.* **6**, 567–584 (2019).

86. Jang, Y.-N. & Baik, E. J. JAK-STAT pathway and myogenic differentiation. *Jak-Stat* **2**, e23282 (2013).

87. Sun, L. *et al.* JAK1-STAT1-STAT3, a key pathway promoting proliferation and preventing premature differentiation of myoblasts. *J. Cell Biol.* **179**, 129–138 (2007).

88. Howard, E. E., Pasiakos, S. M., Blesso, C. N., Fussell, M. A. & Rodriguez, N. R. Divergent Roles of Inflammation in Skeletal Muscle Recovery From Injury. *Front. Physiol.* **11**, 1–13 (2020).

89. Wang, K., Wang, C., Xiao, F., Wang, H. & Wu, Z. JAK2/STAT2/STAT3 are required for myogenic differentiation. *J. Biol. Chem.* **283**, 34029–34036 (2008).

90. Spangenburg, E. E. & Booth, F. W. Multiple signaling pathways mediate LIF-induced skeletal muscle satellite cell proliferation. *Am. J. Physiol. - Cell Physiol.* **283**, 204–211 (2002).

91. Haan, S., Keller, J. F., Behrmann, I., Heinrich, P. C. & Haan, C. Multiple reasons for an inefficient STAT1 response upon IL-6-type cytokine stimulation. *Cell. Signal.* **17**, 1542–1550 (2005).

92. Deng, S. *et al.* Ectopic JAK–STAT activation enables the transition to a stem-like and multilineage state conferring AR-targeted therapy resistance. *Nat. Cancer* **3**, 1071–1087 (2022).

93. Feng, E., Balint, E., Poznanski, S. M., Ashkar, A. A. & Loeb, M. Disease Outcomes. (2021).

94. Dayan, M. *et al.* Effect of aging on cytokine production in normal and experimental systemic lupus erythematosus-afflicted mice. *Exp. Gerontol.* **35**, 225–236 (2000).

95. Sandmand, M. *et al.* Is ageing associated with a shift in the balance between Type 1 and Type 2 cytokines in humans? *Clin. Exp. Immunol.* **127**, 107–114 (2002).

96. Wang, J., Leung, K. S., Chow, S. K. H. & Cheung, W. H. Inflammation and age-associated skeletal muscle deterioration (sarcopaenia). *J. Orthop. Transl.* **10**, 94–101 (2017).

97. Doles, J. D. & Olwin, B. B. The impact of JAK-STAT signaling on muscle regeneration. *Nat. Med.* **20**, 1094–1095 (2014).

98. Nguyen, T., Du, J. & Li, Y. C. A protocol for macrophage depletion and reconstitution in a mouse model of sepsis. *STAR Protoc.* **2**, 101004 (2021).

99. Villas, B. H. Flow cytometry: an overview. *Cell Vis.* **5**, 56–61 (1998).

100. Lee, S. H., Meng, X. W., Flatten, K. S., Loegering, D. A. & Kaufmann, S. H. Phosphatidylserine exposure during apoptosis reflects bidirectional trafficking between plasma membrane and cytoplasm. *Cell Death Differ.* **20**, 64–76 (2013).

101. Perfetto, S. P. *et al.* Amine-reactive dyes for dead cell discrimination in fixed samples. *Curr. Protoc. Cytom.* 1–20 (2010) doi:10.1002/0471142956.cy0934s53.

102. Valieva, Y., Ivanova, E., Fayzullin, A., Kurkov, A. & Igrunkova, A. Senescence-Associated β-Galactosidase Detection in Pathology. *Diagnostics* **12**, (2022).

103. Doura, T. *et al.* Detection of LacZ-Positive Cells in Living Tissue with Single-Cell Resolution. *Angew. Chemie - Int. Ed.* **55**, 9620–9624 (2016).

104. User Manual EdU in vivo Kits. *Base Click, DNA&RNA Expert.* 1–12.

105. Bosselut, R. & Vacchio, M. S. T-cell development: Methods and protocols. *T-Cell Dev. Methods Protoc.* 1–292 (2015) doi:10.1007/978-1-4939-2809-5.

106. Livak, K. J. & Schmittgen, T. D. Analysis of relative gene expression data using real-time quantitative PCR and the 2-ΔΔCT method. *Methods* **25**, 402–408 (2001).

107. Huang, D. W., Sherman, B. T. & Lempicki, R. A. Systematic and integrative analysis of large gene lists using DAVID bioinformatics resources. (2008) doi:10.1038/nprot.2008.211.

108. Juban, G. & Chazaud, B. Efferocytosis during skeletal muscle regeneration. *Cells* **10**, (2021).

109. Wei Shen, Yong Li, Jinhong Zhu, Reto Schwendener, A. J. H. Interaction Between Macrophages, TGF-b1, and the COX-2 Pathway During the Inflammatory Phase of Skeletal Muscle Healing After Injury. *J. Cell. Physiol.* **211(3)**, 736–747 (2008).

110. Liu, X. *et al.* Macrophage depletion impairs skeletal muscle regeneration : the roles. 1–23 (2016).

111. Peng, B. *et al.* BTG2 acts as an inducer of muscle stem cell senescence. *Biochem. Biophys.*

Res. Commun. **669**, 113–119 (2023).

112. Xiao, W., Liu, Y. & Chen, P. Macrophage Depletion Impairs Skeletal Muscle Regeneration: the Roles of Pro-fibrotic Factors, Inflammation, and Oxidative Stress. *Inflammation* **39**, 2016–2028 (2016).

113. Essers, M. A. G. *et al.* IFNα activates dormant haematopoietic stem cells in vivo. *Nature* **458**, 904–908 (2009).

114. Han, S. *et al.* Differential Responsiveness of Monocyte and Macrophage Subsets to Interferon. *Arthritis Rheumatol.* **72**, 100–113 (2020).

115. Sato, T. *et al.* Interferon regulatory factor-2 protects quiescent hematopoietic stem cells from type i interferon-dependent exhaustion. *Nat. Med.* **15**, 696–700 (2009).

116. K. D. KHAN*, KE SHUAIt, GLEN LINDWALL*, STEPHEN E. MAHER*, J. E. DARNELL, J. . & BOTHWELL, A. A. L. M. Induction of the Ly-6A / E gene by interferon a /, 8 and y requires a DNA element to which a tyrosine-phosphorylated 91-kDa protein binds. **90**, 6806–6810 (1993).

117. Talukder, M. A., Menyuk, C. R. & Kostov, Y. Distinguishing between whole cells and cell debris using surface plasmon coupled emission. *Biomed. Opt. Express* **9**, 1977 (2018).

118. Tan, S. C. & Yiap, B. C. DNA, RNA, and protein extraction: The past and the present. *J. Biomed. Biotechnol.* **2009**, (2009).

119. Liu, X. *et al.* IL-6 expression promoted by Poly(I:C) in cervical cancer cells regulates cytokine expression and recruitment of macrophages. *J. Cell. Mol. Med.* **24**, 2284–2293 (2020).

120. Hafner, A. M., Corthésy, B. & Merkle, H. P. Particulate formulations for the delivery of poly(I: C) as vaccine adjuvant. *Adv. Drug Deliv. Rev.* **65**, 1386–1399 (2013).

121. D Yaffe, O. S. Serial passaging and differentiation of myogenic cells isolated from dystrophic mouse muscle. *Nature* (1977).

122. Ahmed M. Abdelmoez, Laura Sardón Puig, Jonathon AB. Smith, Brendan M. Gabriel, Mladen Savikj, Lucile Dollet, Alexander V. Chibalin1, Anna Krook, J. R. Z. & Pillon, and N. J. Comparative profiling of skeletal muscle models reveals heterogeneity of transcriptome and metabolism. *Am J Physiol Cell Physiol* **51**, 204–213 (2019).

123. Manuscript, A. & Myogenesis, R. Interferon resets muscle cell fate by stimulating sequential recrutment. **6**, (2014).

124. Soo M. Ngoi, Michael G. Tovey, and A. T. V. Targeting Poly I:C to the TLR3-independent pathway boosts effector CD8 T cell differentiation through IFNα/β. *Brain Lang.* **88**, 1–20 (2004).

125. Li, Y. G. *et al.* Poly (I:C), an agonist of toll-like receptor-3, inhibits replication of the Chikungunya virus in BEAS-2B cells. *Virol. J.* **9**, 1–8 (2012).

126. Moresi, V., Adamo, S. & Berghella, L. The JAK/STAT pathway in skeletal muscle pathophysiology. *Front. Physiol.* **10**, (2019).

127. Banerjee, S., Biehl, A., Gadina, M., Hasni, S. & Schwartz, D. M. JAK–STAT Signaling as a Target for Inflammatory and Autoimmune Diseases: Current and Future Prospects. *Drugs* **77**, 521–546 (2017).

128. Bivona, J. J. *et al.* Macrophages augment the skeletal muscle proinflammatory response through TNFα following LPS-induced acute lung injury. *FASEB J.* **35**, 1–21 (2021).